UNIVERSIDADE D
COIMBRA

Francisco José Morais Esteves

MODULATION OF ER HOMEOSTASIS AND SEQUESTRATION OF THE TRANSLATION MACHINERY BY MEMBERS OF THE HERPESVIRUS UBIQUITIN-DECONJUGASE FAMILY

VOLUME 1

Dissertação no âmbito do Mestrado em Biologia Celular e Molecular orientada pela Professora Doutora Maria Grazia Masucci e apresentada à Faculdade de Ciências e Tecnologia da Universidade de Coimbra.

julho de 2022

Master's Degree in Cellular and Molecular Biology
Dissertation in Cellular and Molecular Biology

Francisco José Morais Esteves

Modulation of ER homeostasis and sequestration of the translation machinery by members of the herpesvirus ubiquitin-deconjugase family

Supervisor: Maria Grazia Masucci
Co-Supervisor: Jiangnan Liu
DCV Tutor: Isabel da Silva Henriques

Maria G. Masucci's Group
Department of Cell and Molecular Biology
Karolinska Institutet, Stockholm, Sweden

July 2022

Index

Abstract

Herpesviruses are a large family of viruses that are capable to establish life-long non-productive infections in their hosts, the transmission to new hosts being dependent on reactivation and initiation of a productive infection. During productive replication, the endoplasmic reticulum (ER) is inundated with herpesviral proteins and the accumulation of unfolded proteins in the ER lumen activates the unfolded protein response (UPR). This stress response aims to restore protein homeostasis through translational and transcriptional reprogramming or, if homeostasis cannot be restored, it leads the cell death apoptosis. In addition, the translation of viral proteins during productive infection often causes ribosome stalling and collisions, which are readily sensed by co-translational surveillance mechanisms, including the ribosome quality control (RQC) pathway. When ribosome stall during co-translational translocation of proteins to the ER, a specialized branch of the RQC is activated, the ER-RQC, which unclogs the translocon by targeting the nascent polypeptide for lysosomal degradation. To create an optimal niche for replication, herpesviruses have developed strategies to usurp cellular stress responses. Since most of these cellular pathways are regulated by the covalent attachment of ubiquitin-like polypeptides (UbLs), herpesviruses have included in their protein repertoire deconjugating enzymes (DUBs) that can modulate the outcome of cellular stress responses.

Here, I have found that the DUBs encoded in the N-terminal domain of the large tegument proteins of Epstein-Barr virus (EBV), human cytomegalovirus (HCMV) and Kaposi's sarcoma associated herpesvirus (KSHV) inhibit the conjugation of the UbL UFM1 (ubiquitin-fold modifier-1) to the ribosomal subunit RPL26, which participates in the activation of the ER-RQC pathway. Inhibition of the ER-RQC by the viral DUBs correlated with activation of the UPR, increased phosphorylation of the translation initiation factor eIF2α and upregulation of the stress response regulator ATF4. These findings highlight a possible role of the viral DUBs in the regulation of protein translation and ER stress responses, which may favour the synthesis of viral proteins and promote cell survival during productive infection.

Resumo

Os herpesvírus são uma grande família de vírus que são capazes de estabelecer infeções não produtivas ao longo da vida dos seus hospedeiros, sendo a transmissão para novos hospedeiros dependente da reativação e início de uma infeção produtiva. Durante a replicação produtiva, o retículo endoplasmático (ER, do inglês: *endoplasmic reticulum*) é inundado com proteínas virais e a acumulação de proteínas não-enoveladas no lúmen do ER ativa a resposta a proteínas não-enoveladas (UPR, do inglês: *unfolded protein response*). Esta resposta ao stress visa restaurar a homeostase proteica por meio de reprogramação traducional e transcricional ou, caso a homeostase não possa ser restabelecida, levar à morte da célula por apoptose. Além disso, a tradução de proteínas virais durante a infeção produtiva geralmente causa paralisação e colisões de ribossomas, que são prontamente detetadas por mecanismos de vigilância co-traducionais, incluindo a via de controlo de qualidade de ribossomas (RQC, do inglês: *ribosome quality control*). Quando o ribossoma para durante a translocação co-traducional de proteínas para o ER, um ramo especializado do RQC é ativado, o ER-RQC. Esta resposta permite a desobstrução do translocão ao conduzir a cadeia polipeptídica nascente à degradação lisossomal. De modo a criar um nicho ideal para a replicação, os herpesvírus desenvolveram estratégias para usurpar as respostas celulares ao stress. Como a maioria dessas vias celulares é regulada pela ligação covalente de polipéptidos semelhantes à ubiquitina (UbLs, do inglês: *ubiquitin-like polypeptides*), os herpesvírus incluem enzimas desconjugantes (designadas, genericamente, deubiquitinases ou DUBs) no seu reportório proteico que podem modular o resultado das respostas celulares ao stress.

Neste projeto descobri que as DUBss codificadas no domínio N-terminal das grandes proteínas do tegumento dos vírus Epstein-Barr (EBV), citomegalovírus humano (HCMV) e herpesvírus do sarcoma de Kaposi (KSHV) inibem a conjugação do UbL UFM1 (do inglês: *ubiquitin-fold modifier-1*) à subunidade ribossomal RPL26, que participa na ativação da via ER-RQC. A inibição do ER-RQC pelos DUBs virais encontra-se relacionada com ativação da UPR, aumento da fosforilação do fator de iniciação da tradução eIF2α e acumulação do regulador de resposta ao stress ATF4. Estas descobertas destacam um possível papel das DUBs virais na regulação da tradução de proteínas e respostas ao stress do ER, o que pode favorecer a síntese de proteínas virais e promover a sobrevivência da célula durante a infeção produtiva.

Introduction

Ubiquitin-like polypeptides signalling networks

Ubiquitin-like polypeptides (UbLs) are a family of posttranslational modifiers (PTMs) that provide a flexible means to orchestrate a plethora of cellular processes by controlling the activity, function, stability and localization of modified substrates. All UbLs are small polypeptides that share a β-grasp fold organization consisting of a mixed β-sheet structure with a central α-helix **(Hochstrasser, 2009)**. To date, seventeen UbLs have been identified in humans: ubiquitin (Ub), small ubiquitin-related modifiers (SUMO)-1, -2 and -3, NEDD8 (neural precursor cell expressed, developmentally downregulated-8), ISG15 (interferon-stimulated gene-15), UFM1 (ubiquitin-fold modifier-1), URM1 (ubiquitin-related modifier-1), FAT10 (HLA-F adjacent transcript 10), MNSFβ (monoclonal nonspecific suppressor factor β) and the LC3 (microtubule-associated light chain) and GABARAP (γ-amino-butyric acid receptor-associated protein) family of modifiers **(van der Veen & Ploegh, 2012)**. Diverse interaction surfaces are formed after the attachment of single UbLs or topologically different poly-UbL chains to substrates. Consequently, this diversity is recognized by signal transducers containing dedicated binding domains, which, in the end, permits the generation of a broad spectrum of signals that lead to the engagement of the modified substrate in specialized cellular functions **(Hurley *et al.*, 2006)**.

The covalent attachment of UbLs to substrates relies on a dedicated enzymatic cascade that starts with the processing of a UbL precursor by a specific protease, which exposes a reactive C-terminal Gly necessary for conjugation. Following this initial step, an activating enzyme (E1) adenylates and forms a high-energy thioester bond with the C-terminal Gly of the mature UbL, followed by loading on the catalytic Cys of a conjugating enzyme (E2). The E2 then transfers the UbL to its final substrate with the help of substrate-specific ligating enzyme (E3). Like other posttranslational modifications, UbL signalling networks can be regulated by the action of deconjugating enzymes (collectively referred to as DUBs), which hydrolyse the covalent bond between the UbL and the substrate **(Kerscher *et al.*, 2006)**.

In the next section, I will overview the current knowledge on UFM1 and its (de)conjugating enzymes and substrates.

Ubiquitin-fold modifier-1 (UFM1) and UFMylation substrates

Ubiquitin-fold modifier-1 (UFM1) is an 85-amino acid protein of 9.9 kDa and the most recently discovered member of the UbLs family. Having been initially identified as an important PTM during embryonic development, novel biological functions have slowly been unravelled. These include important roles in autophagy, transcriptional

regulation, DNA damage and, more recently, ER stress response. Although UFM1 resembles Ub in the tertiary structure, the sequences display very low similarity, making UFM1 and its dedicated enzymatic cascade a unique and highly specialized UbL **(Komatsu *et al.*, 2004; Witting & Mulder, 2021)**.

Similar to other UbLs, the attachment of UFM1 to specific substrates, UFMylation, is dependent on a sequence of reactions mediated by three enzymes: the E1-activating enzyme UBA5, the E2-conjugating enzyme UFC1 and the scaffold-type E3-ligating enzyme UFL1 **(Komatsu *et al.*, 2004; Tatsumi *et al.*, 2010)**. The reversibility of the process is ensured by the action of the UFM1-specific Cys protease UFSP2 (UFM1 specific peptidase 2). The latter is also responsible for the cleavage of the UFM1 precursor (proUFM1), thus exposing a reactive C-terminal Val-Gly motif by removal of the last two amino acids (Ser-Cys) **(Ishimura *et al.*, 2017)**. Thereafter, UBA5 adenylates and binds the reactive C-terminal Gly of UFM1 through a high energy thioester linkage. Next, UBA5 transfers the activated UFM1 to UFC1 in a trans-thiolation reaction **(Habisov *et al.*, 2016; Padala *et al.*, 2017)**. Finally, the UFM1 is conjugated to a Lys residue of protein substrates with the help of a scaffold-type E3 ligase complex, composed by UFL1 and its adaptor proteins, DDRGK1 and CDK5RAP3. Lacking a transmembrane domain, UFL1 requires DDRGK1 to be recruited to the ER membrane. Interestingly, DDRGK1 is itself modified by UFM1, thus controlling its binding activity to UFL1 and, ultimately, the ligase activity **(Yoo *et al.*, 2014; Lemaire *et al.*, 2011; Liang *et al.*, 2020)**. Initially identified as being involved in DNA damage and cell cycle control, CDK5RAP3 has been demonstrated to co-localize with UFL1 and DDRGK1, ensuring the subcellular localization of the ligase, as well as promoting its stability by regulating its degradation **(Wu *et al.*, 2010; Lemaire *et al.*, 2011; Liang *et al.*, 2020)**. Containing multiple Lys residues in its structure, UFM1 can polymerize and form topologically different chains that can target the substrates to various fates and cellular functions. Although still not completely understood, previous reports have pointed to a decisive role of CDK5RAP3 in poly-UFMylation **(Walczak *et al.*, 2019)**.

The slowly expanding list of UFM1 substrates include, in addition to DDRGK1 **(Tatsumi *et al.*, 2010)**, the activating signal co-integrator 1 (ASC1) **(Yoo *et al.*, 2014)**, the DNA repair protein MRE11 **(Wang *et al.*, 2019)**, the ribosomal protein RPL26 **(Walczak *et al.*, 2019; Liang *et al.*, 2020; Wang *et al.*, 2020)**, ribophorin I (RPN1) **(Liang *et al.*, 2020)** and the tumour suppressor protein p53 **(Liu *et al.*, 2020)**.

In the next section, I will highlight some of the recently discovered roles of UFMylation in the modulation of ER and ribosomal stress responses.

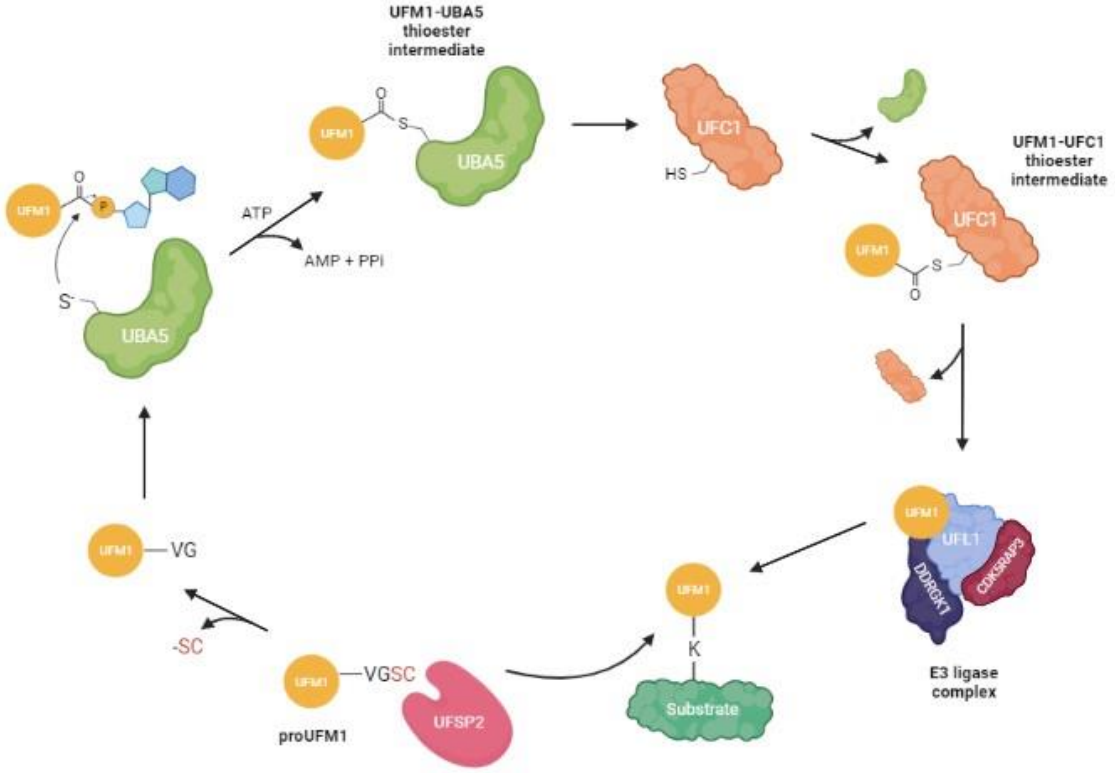

Figure 1. Schematic overview of the UFM1 cascade. In a first step, the UFM1-specific protease and deUFMylase UFSP2 cleaves the last two C-terminal amino acids (Ser-Cys) of proUFM1, thus exposing a catalytic active Gly that is necessary for conjugation. Next, the E1 UBA5 activates the mature UFM1 through a high energy thioester bond in an ATP-dependent manner. In a trans-thiolation reaction, UBA5 transfers UFM1 to the E2 UFC1, which, together with the scaffold-type E3 UFL1, catalyses the attachment of UFM1 to Lys residues of protein substrates. The adaptor proteins DDRGK1 and CDK5RAP3 co-localize with UFL1, regulating the activity and the ER localization of the ligase. UFM1 can be hydrolysed from modified substrates by the action of UFSP2.

UFM1 and ER stress

The ER consists of a dynamic network of flat sheets and curved tubules and is responsible for the assembly and proper folding of proteins in the secretory pathway, which accounts for approximately 30% of the cellular proteome. Increased protein secretion or accumulation of unfolded or misfolded proteins in the ER lumen may constitute a threat to its secretory capacity and other ER functions – a condition referred to as ER stress. To restore homeostasis, the unfolded protein response (UPR), the ER-associated degradation pathway (ERAD) and ER-phagy are activated. The UPR upregulates the translation of ER chaperones to increase protein folding. At the same time, the ER network expands and the ERAD pathway is activated. ERAD mediates the extraction of unfolded or misfolded proteins from the ER followed by their degradation

in the cytosol by the ubiquitin-proteasome system. Under chronic stress or irreversible damage, the UPR may switch its signalling toward an apoptosis programme **(Hetz *et al.*, 2020)**.

The UPR is branched in three signalling pathways initiated by the ER transmembrane protein sensors IRE1α (inositol-requiring transmembrane kinase/endoribonuclease 1α), ATF6α (activating transcription factor α) and PERK (PKR-like ER kinase). The PERK sensor is a kinase that phosphorylates eukaryotic translation initiation factor 2 subunit-α (eIF2α), leading to translation attenuation and reduced influx of newly synthesized proteins into the ER. This response to ER stress is essential to avoid overloading the ER with misfolded proteins. However, phosphorylated eIF2α specifically upregulates the translation of ATF4 (activating transcription factor 4), a stress-inducible transcription factor that activates the expression of cytoprotective genes involved in amino acid biosynthesis the antioxidative response and autophagy, including the gene *CHOP* (CCAAT-enhancer-binding protein homologous protein). The phosphorylation of eIF2α is also promoted by PKR (protein kinase double-stranded RNA-dependent) and GCN2 (general control non-derepressible-2) **(Donnelly *et al.*, 2013)**. In parallel, the IRE1α sensor, a protein kinase/endoribonuclease, oligomerizes and is autophosphorylated, promoting the splicing of the transcription factor XBP1 (X-box binding protein 1) messenger RNA (mRNA). The spliced XBP1 mRNA encodes the transcription factor sXBP1 that upregulates the expression of ER chaperones and activates the ERAD. IRE1α endoribonuclease activity on small mRNAs or precursor microRNAs (miRNAs) also contributes to lower mRNA abundance, a process commonly referred to as IRE1-dependent decay (RIDD).

The UFM1 signalling network was found to be intimately related to the UPR. For example, disturbance of ER homeostasis and inhibition of vesicle trafficking led to transcriptional upregulation of UFM1 and the UFM1-associated enzymatic machinery. This was attributed to binding of the transcription factor XBP1 to the UFM1 promoter **(Zhang *et al.*, 2012; Zhu *et al.*, 2019)**. Additionally, mice impaired for UFMylation showed increased activity of the UPR, including activation of the sensors IRE1α and PERK, together with higher levels of XBP1 translation, eIF2α phosphorylation and *CHOP* transcription **(Cai *et al.*, 2015; Zhang *et al.*, 2015; Gerakis *et al.*, 2019)**. Although some enlightening studies have been published in the past years, the mystery of the interaction between UPR and the UFM1 cascade is far from being solved.

UFM1 and aberrant translation

Ribosomes are powerful decrypting machines that translate mRNA-embedded information into polypeptide chains, which become functional proteins. Abnormal mRNA (*e.g.*, polyadenylated residues) and ribotoxic stressors (*e.g.*, translation inhibitors, amino acids starvation, infection) can lead to the stalling and collision of ribosomes **(Park *et al.*, 2021)**.

In a scenario of moderate ribosomal collisions, stalled ribosomes are recycled, and aberrant translation intermediates are degraded by the ribosome-associated quality control (RQC) pathway, which is initiated by the ubiquitination of ribosome small subunit proteins (*e.g.*, RPS2, -3, -10 and -20) by the E3 Ub ligase ZNF598. This process can be reverted by the deubiquitinating enzymes OTUD3 (ovarian tumour deubiquitinase-3), USP10 and USP21 **(Garshott *et al.*, 2020; Meyer *et al.*, 2020)**. Ubiquitination of ribosome small subunit proteins allows the recruitment of either the RQC-trigger (RQT) or the PELO-HBSL1-ABCE1 protein complexes, which promotes the dissociation of the ribosome large and small subunits **(Pisareva *et al.*, 2011)**. Proteasomal degradation of the nascent chain associated with the disassembled large subunit occurs after recognition by NEMF (nuclear export mediator factor) and the recruitment of the E3 Ub ligase LTN1 (listerine 1) **(Joazeiro, 2019)**. A different strategy is adopted during translation of ER-bound proteins that are co-translationally translocated into the ER. This process often results in ribosomal stalling, translocon clogging and accumulation of arrested products in the ER. In order to preserve ER homeostasis, an alternative RQC pathway (ER-RQC) senses ribosomal stalling at the ER and UFMylates RPL26, a large subunit protein located near the peptide exit tunnel, which destabilizes the stalled nascent chain and targets it for lysosomal degradation **(Wang *et al.*, 2020)**.

In addition, after a threshold of ribosomal collisions is reached, the cell activates the integrated stress response (ISR) pathway. During ISR, elF2α phosphorylation is increased by activation of the kinase GCN2, which results in the shutdown of general translation. Anisomycin (ANS) is a drug that directly affects the ribosomal peptidyl transferase activity, which leads to GCN2-dependent phosphorylation of eIF2α **(Wu *et al.*, 2020)**.

Herpesviruses deconjugases

Being obligatory intracellular parasites, viruses have evolved ingenious strategies to modulate the cellular environment, turning it propitious to their own replication and spread. These strategies include hijacking the molecular machinery of the host cell and escaping the cellular and organismal defences that are triggered by infection. It is, therefore, not surprising that viruses have developed means to target UbLs signalling networks, since these commandeer a multitude of cellular functions that ultimately impact the outcome of infection. Common strategies to interfere with these pathways involve altering the expression of host deconjugases, redirecting the activity of the cellular enzymes towards new cellular or viral substrates or even encoding their own deconjugases. Herpesviruses are a good example of viruses that take advantage of these cellular signalling networks, since all herpesviruses studied to date encode, at least, one deconjugase **(Masucci, 2021)**.

The *Herpesviridae* are a large family of double-stranded DNA viruses that encompasses seven human pathogens: the α-herpesviruses Herpes simplex virus-1 and -

2 (HSV-1 and -2; HHV-1 and -2) and Varicella zoster virus (VZV; HHV-3); the β-herpesviruses Human cytomegalovirus (HCMV; HHV-5) and Human herpesvirus-6 and -7 (HHV-6 and -7); the γ-herpesviruses Epstein-Barr virus (EBV; HHV-4) and Kaposi sarcoma herpesvirus (KSHV; HHV-8). All herpesviruses share the ability to establish latent infections in their hosts, being able to reactivate and initiate a productive cycle. To survive in a latent state, herpesviruses need to circularize their genomes to form episomes and to modulate the cell environment in their favour, while expressing a very limited set of genes, in order to avoid elimination by the host immune response **(Cohen, 2020)**.

All herpesviruses studied to date encode deconjugases embedded in the N-terminal domain of the large tegument proteins. These proteins are expressed during the late phase of the productive infection and contain a strictly conserved Cys-His-Asp catalytic triad in the first N-terminal 280 amino acids **(Schlieker *et al.*, 2005)**. Deconjugases encoded by herpesviruses have been shown to cleave with similar efficiency Ub and NEDD8 conjugates, but not ISG15 **(Gastaldello *et al.*, 2010)**. Within the list of viral DUBs encoded by herpesviruses are UL36 (HSV-1 and -2), UL48 (HCMV), BPLF1 (EBV) and ORF64 (KSHV) **(Masucci, 2021)**.

EBV-encoded BPLF1 has attracted much attention over the past years because several aspects of the pathophysiology of EBV infection have been found to be dependent on its DUB activity. In the next section, I will direct my attention to BPLF1, as well as the viral and cellular substrates of its DUB domain.

BPLF1: EBV's Swiss army knife of infection

EBV is an immunogenic and oncogenic human virus that is estimated to establish life-long infections in, at least, 90% of the adult population, which makes it the most ubiquitous human virus worldwide **(de-Thé *et al.*, 1975)**. Primary infection may lead to the development of infectious mononucleosis (IM), especially in adolescents. Although after a primary infection the large majority of the virus carriers remain asymptomatic, several malignancies have been linked to EBV persistence in the infected host, especially in immunocompromised individuals. The most prominent are nasopharyngeal carcinoma, gastric carcinoma, Hodgkin lymphoma, Burkitt lymphoma, diffuse large B-cell lymphoma and extranodal NK/T-cell lymphoma, nasal type **(Shannon-Lowe & Rickinson, 2019)**. A recent review estimated that EBV-related cases from these six pathologies were attributed to 293.700-357.900 new cases and 137.900-208.700 deaths in 2020 **(Wong *et al.*, 2022)**. Recently, EBV infection was implicated as a risk factor of multiple sclerosis **(Houen *et al.*, 2020)**.

Similar to other herpesviruses, EBV establishes both latent and a lytic/productive infection, characterized by distinct gene expression programmes and replication strategies. In latency, only a restricted set of viral proteins and non-coding RNAs (ncRNAs) are expressed, allowing the virus to persist silently in proliferating B cells **(Babcock *et al.*, 1998)**. Spontaneously triggered or following exogenous induction, the lytic/productive cycle is characterized by the coordinated expression of immediate early,

early and late viral proteins, which leads to virion production and death of the infected cells **(Hammerschmidt & Sugden, 2013)**.

BPLF1 is the largest tegument protein (3149 amino acids) of EBV. It is expressed during the late phase of the lytic cycle, but transcripts are detected as early as 6 to 8 h after infection **(Gastaldello *et al.*, 2010)**. After translation, BPLF1 is incorporated into the tegument of viral particles that can be subsequently released into newly infected cells **(van Gent *et al.*, 2014)**. Experiments using BPLF1 knockdown or silencing have shown that this protein is essential for EBV replication **(Whitehurst *et al.*, 2009; Gastaldello *et al.*, 2010)**. van Gent *et al.* have demonstrated that BPLF1 is an active DUB in EBV-infected B cells **(van Gent *et al.*, 2014)**. Infecting a humanized mouse model with EBV $BPLF1^{WT}$ or $BPLF1^{KO}$ demonstrated that this viral protein is determinant for EBV infectivity and pathogenesis, namely human B-cell transformation and tumour formation **(Whitehurst *et al.*, 2015)**.

An interesting feature of this protein is its Ub and NEDD8 deconjugase activity within the first 205 amino acids of the N-terminal region and strictly conserved across all members of the *Herpesviridae* family **(Gastaldello *et al.*, 2010)**. The DUB activity is centred on a catalytic triad composed of Cys-His-Asp and mutation of the active-site Cys results in complete loss of enzymatic activity **(Whitehurst *et al.*, 2009)**. BPLF1 DUB domain is active against both Lys63 and Lys48 polyubiquitin chains, suggesting that this protein may have both regulatory functions and a role in rescuing proteins from degradation **(Whitehurst *et al.*, 2009)**.

During the past decade, several cellular substrates have been identified. Among these are several cellular substrates, such as Cul1, -2, -3, -4A, -4B, -5 **(Gastaldello *et al.*, 2012)**, PCNA **(Whitehurst *et al.*, 2012)**, Rad6/18 **(Kumar *et al.*, 2014)**, Polη **(Dyson *et al.*, 2017)**, TOP2 **(Li *et al.*, 2021)**, TRAF6 **(Saito *et al.*, 2013)**, NEMO **(van Gent *et al.*, 2014)**, IκBα **(van Gent *et al.*, 2014)**, 14-3-3 **(Gupta *et al.*, 2018)**, TRIM25 **(Gupta *et al.*, 2019)** and SQSTM1/p62 **(Ylä-Anttila *et al.*, 2021)**; however, only one viral substrate has been identified to date - the small subunit of the viral ribonucleotide reductase (RR2) **(Whitehurst *et al.*, 2009)**.

Aim of the project

Using mass spectrometry analysis, our group has previously built an EBV-BPLF1 interactome with cellular proteins **(Gupta *et al.*, 2018)**. An in-depth analysis of the interactome has identified several components of the ribosome and protein translation machinery, including the UFM1 E3 ligase UFL1, the ribosomal protein RPL26 and the translation initiation factor eIF2α, as putative BPLF1 interacting partners **(manuscript in preparation)**. Hence, in this study we aimed to determine whether the DUB encoded in the N-terminal domain of BPLF1 has the capacity to:

- Interfere with the UFM1 conjugation/deconjugation cascade.
- Disturb downstream effects of this posttranslational modification (*e.g.*, modulation of ER homeostasis and hijacking of translation machinery).
- Share these activities with DUB homologues encoded by other members of the *Herpesviridae* family.

Results

BPLF1, UL36, UL48 and ORF64 DUB domains bind to a ubiquitin probe

Initially, the activity of the DUBs encoded in the N-terminal domains of the large tegument proteins of EBV, HSV-1 and -2, HCMV and KSHV was tested. HeLa cells were transiently transfected for 24 h with previously produced recombinant plasmids expressing the FLAG-tagged versions of EBV's BPLF1 (FLAG-BPLF1), HSV-1's UL36 (FLAG-UL36), HCMV's UL48 (FLAG-UL48) and KSHV's ORF64 (FLAG-ORF64) **(Gastaldello *et al.*, 2010)**. A FLAG-tagged version of a BPLF1 inactive mutant, where the catalytic Cys61 was substituted with Ala, was included (FLAG-BPLF1^{C61A}). Lysates of the transfected HeLa cells were subsequently incubated with a ubiquitin probe (HA-Ub-VS). The reactive vinyl-sulphone (VS) moiety of the probe promotes the formation of a covalent bond with the catalytic Cys residue of DUBs, which is detected in western blots as a shift in molecular weight corresponding to the size of the probe. Inactive DUBs were expected to fail to form complexes with HA-Ub-VS, which would result in the presence of a single band in the FLAG tag blot, corresponding to the free form of the DUB. As expected, incubation with HA-Ub-VS resulted in a ~ 10 kDa shift of all viral proteins except for the catalytic mutant BPLF1^{C61A}. These results confirm that the plasmids used in these experiments expressed catalytically active herpesviral DUBs **(Figure 2)**.

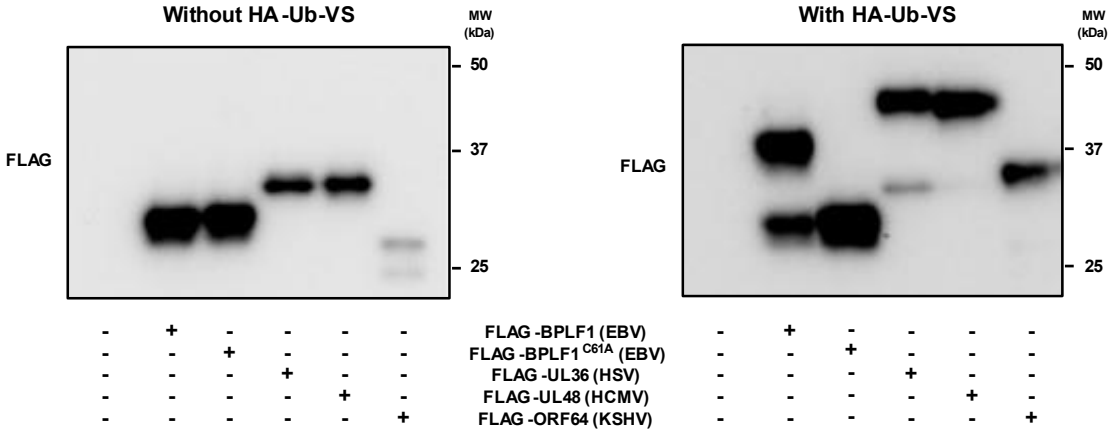

Figure 2. BPLF1, UL38, UL48 and ORF64 DUB domains form complexes with ubiquitin. HeLa cells were transiently transfected for 24 h with plasmids expressing FLAG-BPLF1, FLAG-BPLF1^{C61A}, FLAG-UL36, FLAG-UL48, FLAG-ORF64 or the FLAG empty vector. Cells were lysed with NP40 lysis buffer supplemented with protease inhibitors and cell lysates were incubated without ***(left panel)*** or with the ubiquitin probe HA-Ub-VS ***(right panel)*** for 1 h at 37 ºC. Western blots were probed with an antibody to FLAG. The presence of HA-Ub-VS resulted

in the formation of complexes of Ub with all viral DUBs tested except BPLF1^{C61A}, confirming their activity.

BPLF1 interacts with UFL1

To investigate whether the EBV-encoded DUB interacts with the E3 ligase UFL1, which participates in the last step of the UFMylation cascade, HeLa cells were transiently transfected with FLAG-tagged versions of the N-terminal catalytic domain of BPLF1 and the catalytically inactive mutant BPLF1^{C61A}. Then, lysates of the transfected HeLa cells were immunoprecipitated with antibodies recognizing the FLAG tag or UFL1. UFL1 was readily detected in western blots of the FLAG immunoprecipitates, independent of the catalytic activity of BPLF1 **(Figure 3, *left panel*)**. Conversely, both BPLF1 and BPFL1^{C61A} co-immunoprecipitated with UFL1. BPLF1^{C61A} was strongly enriched in UFL1 immunoprecipitates compared to BPLF1 **(Figure 3, *right panel*)**. However, caution should be used in the interpretation of this finding since both overexpression and immunoprecipitation of BPLF1^{C61A} were expressed at higher levels compared to wild type BPLF1. Nevertheless, the data support the conclusion that BPLF1 interacts with UFL1 in cells and the inactivating C61A mutation does not significantly affect the efficiency of the interaction.

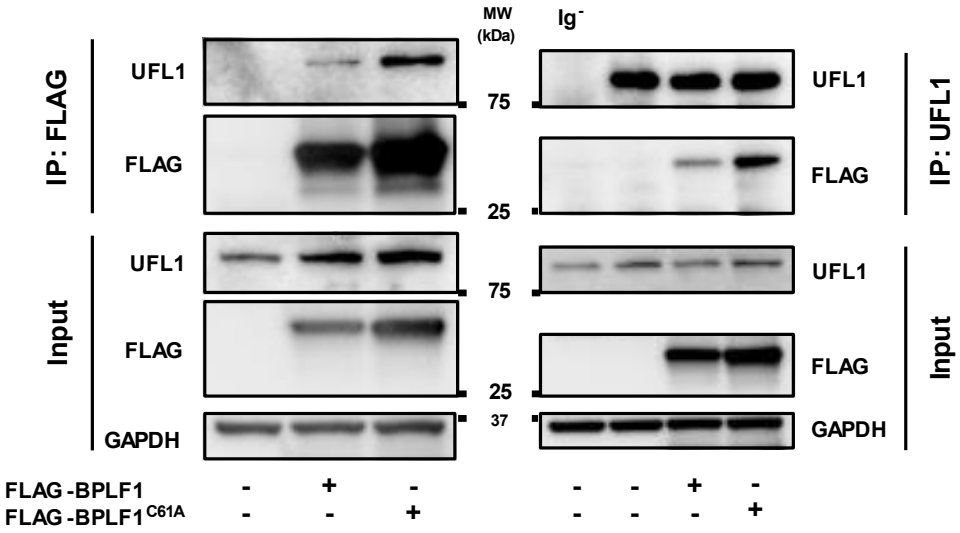

Figure 3. BPLF1 interacts with UFL1 independently of its catalytic activity. HeLa cells were transiently transfected for 48 h with plasmids expressing FLAG-BPLF1, FLAG-BPLF1^{C61A} or the FLAG empty vector. Cells were lysed with NP-40 lysis buffer supplemented with DUB and protease inhibitors. FLAG tag and UFL1 were immunoprecipitated from cell lysates under native conditions and western blots were probed with antibodies to UFL1, FLAG and GAPDH. BPLF1 and BPLF1^{C61A} were readily detected in UFL1 immunoprecipitates in a similar amount. The same interaction was validated in FLAG immunoprecipitates. Western blots of one representative experiment out of two are shown in the figure.

BPLF1 impairs RPL26 UFMylation

Since BPLF1 interacts with the UFM1-specific E3 ligase UFL1, the following step was to investigate if BPLF1 affected the UFMylation of endogenous proteins. HeLa cells were transiently transfected with FLAG-BPLF1 and FLAG-BPLF1^{C61A} followed by treatment with ANS for 1 h to induce UFMylation **(Figure 4A)**. ANS is a modest ribotoxic stressor that inhibits translation elongation by preventing peptidyl transferase activity, thus promoting ribosome stalling and RPL26 UFMylation **(Garreau de Loubresse *et al.*, 2014; Wang *et al.*, 2020)**. Cells transfected with FLAG-BPLF1 clearly presented lower levels of ANS-induced UFMylation, whereas FLAG-BPLF1^{C61A} led to an equal or slightly higher UFM1 signal compared to the ANS-treated control, suggesting that BPLF1 catalytic activity somehow impairs UFMylation of cellular substrates. Given that RPL26 was previously identified as the principal target of UFMylation **(Walczak *et al.*, 2019)** and knowing that RPL26 is part of the BPLF1 interactome, we asked whether BPLF1 affected RPL26 UFMylation. HeLa cells transiently transfected with a c-Myc-tagged version of RPL26 (RPL26-Myc), FLAG-BPLF1 or FLAG-BPLF1^{C61A} were treated or not with ANS for 1 h followed by immunoprecipitation with anti-c-Myc agarose beads **(Figure 4B)**. While FLAG-BPLF1^{C61A} had little effect on the levels of mono- (~ 27 kDa) and di- (~ 36 kDa) UFMylated RPL26, BPLF1 abolished RPL26-conjugated UFM1 bands.

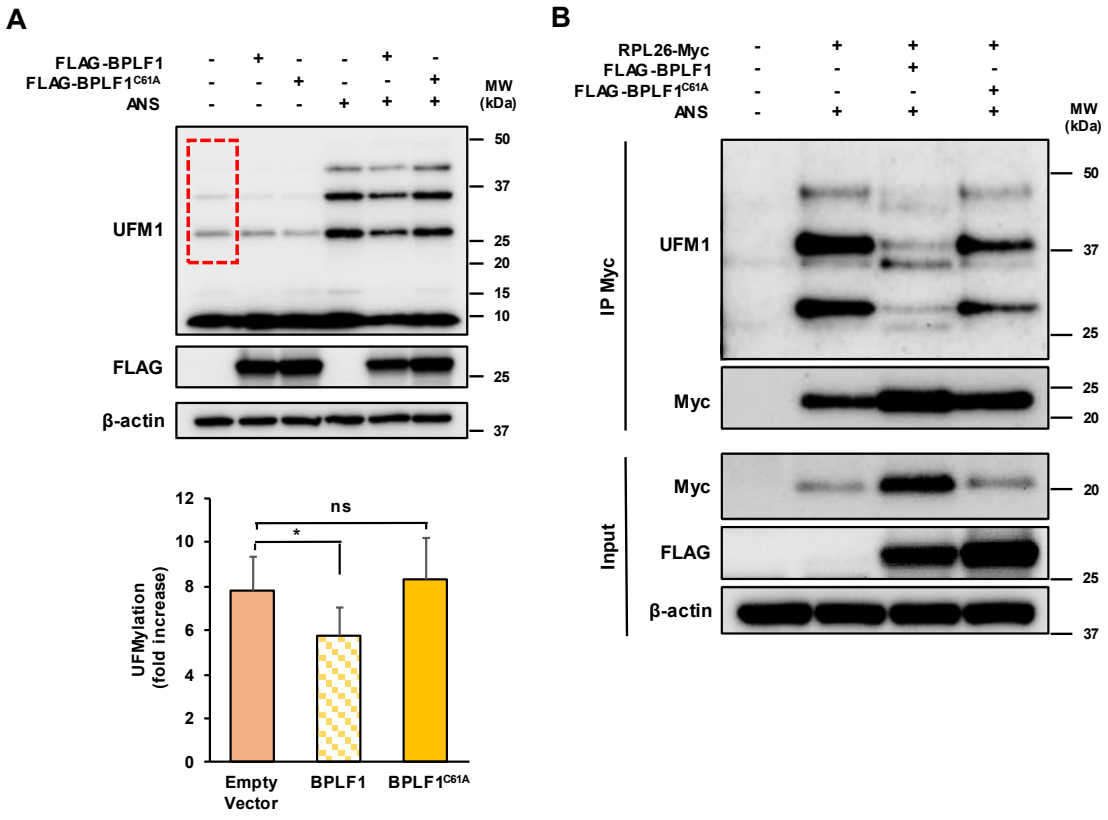

Figure 4. BPLF1 disturbs RPL26 UFMylation in a scenario of ribosome stalling. (A) HeLa cells were transiently transfected for 48 h with plasmids expressing FLAG-BPLF1, FLAG-BPLF1^{C61A} or FLAG empty vector and treated or not with ANS 200 nM for 1 h. Cells were lysed with RIPA lysis buffer supplemented with DUB and protease inhibitors and western blots were probed with antibodies to UFM1, FLAG and β-actin. The expression of BPLF1 decreases endogenous UFMylation after induction of ribosome stalling by ANS, while BPLF1^{C61A} expression slightly increased endogenous UFMylation. Western blots from one representative experiment out of three are shown in the figure. Quantification of UFM1 fold increase after ANS treatment was done using the Image Lab software and the intensity of the UFM1 signal was obtained by demarking the area occupied by the ubiquitously observed three band-patterns, as indicated by the red rectangle in the blot. The mean ± SD of three experiments is shown. Statistical analysis was performed using Student's *t*-test: ns = $P > 0.05$, * = $P \leq 0.05$. **(B)** HeLa cells were transiently co-transfected for 48 h with plasmids expressing RPL26-Myc and FLAG-BPLF1, FLAG-BPLF1^{C61A} or the FLAG empty vector and treated or not with ANS 200 nM for 1 h. Cells were lysed with NP40 lysis buffer supplemented with DUB and protease inhibitors. RPL26-Myc was immunoprecipitated from cell lysates under native conditions. Western blots were probed with antibodies to UFM1, Myc, FLAG and β-actin. The expression of BPLF1 clearly abrogates RPL26 UFMylation, while the effect of BPLF1^{C61A} is considerably minor. Western blots from one representative experiment out of two are shown in the figure.

This result strongly indicates that catalytically active BPLF1 impairs RPL26 UFMylation. Band patterns of similar molecular weights were observed in UFM1 blots of both experiments **(Figures 4A and 4B)**, confirming that the bands observed in **Figure 4A** correspond to UFMylated forms of RPL26. As in previous reports, a strong band with ~ 45 kDa appeared in both UFM1 blots; although its molecular weight suggests the existence of a tri-UFMylated form of RPL26, this hypothesis has not yet been confirmed **(Wang *et al.*, 2020)**. Altogether, the evidence points to the capacity of BPLF1 catalytic activity to impair RPL26 UFMylation and, eventually, the activation of the ER-RQC pathway. Whether this effect is due to direct deUFMylation of RPL26 or is mediated by the capacity of BPLF1 to interfere with upstream events in the RPL26 UFMylation cascade remains to be elucidated.

BPLF1 activates the UPR pathway

Since the UFMylation of RPL26 was shown to be required for activation of the ER-RQC to maintain ER homeostasis and prevent triggering of the UPR **(Gerakis *et al.*, 2019)**, the following question was if the capacity of catalytically active BPLF1 to inhibit RPL26 UFMylation correlates with activation of the UPR. To investigate whether BPLF1 affects this cellular response, HeLa cells were transiently transfected with FLAG-BPLF1 and FLAG-BPLF1^{C61A} or, as control, treated with thapsigargin (TPG) **(Figure 5B)**. TPG is an ER stressor that depletes the Ca^{2+} store in the ER and activates the UPR **(Lindner *et al.*, 2020)**. As expected, cells treated with TPG presented higher levels of

phosphorylated eIF2α (p-eIF2α), ATF4 and CHOP compared to the negative control, therefore validating TPG as an activator of the PERK pathway. The levels of ATF4 and CHOP were higher in cells transfected with FLAG-BPLF1 than in cells treated with TPG. This effect was dependent on the catalytic activity of BPLF1, since the levels of p-eIF2α, ATF4 and CHOP were significantly lower in cells transfected with FLAG-BPLF1^{C61A}. Overall, these results establish BPLF1 as a potent activator of the UPR. However, the *modus operandi* of BPLF1 catalytic activity in the activation of the PERK pathway and whether it can also trigger other arms of the UPR remain to be clarified.

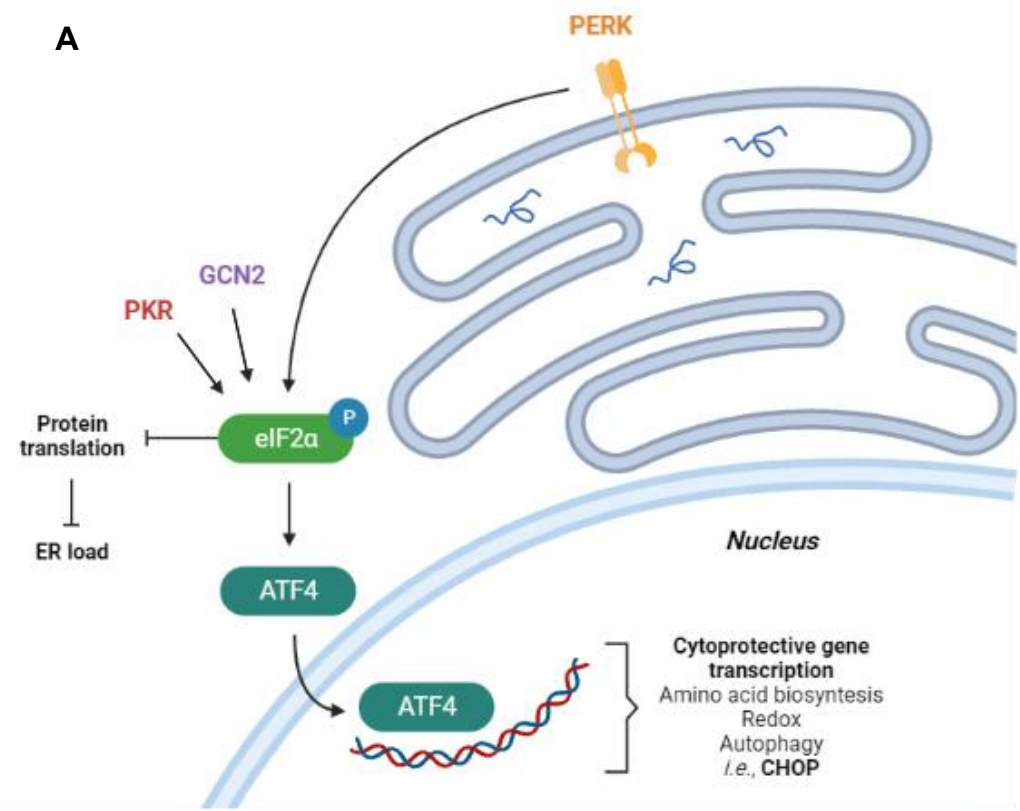

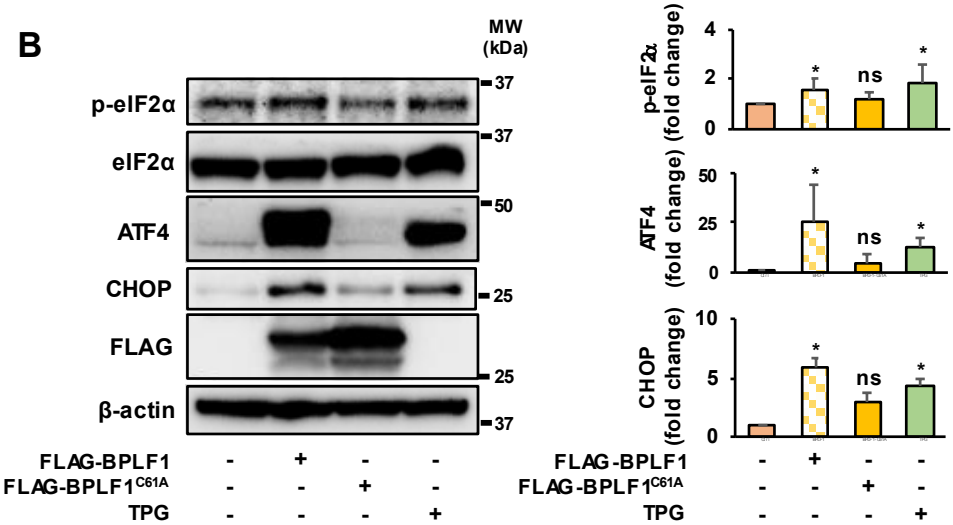

Figure 5. BPLF1 activates the PERK pathway of the UPR. (A) Schematic representation of the PERK branch of the UPR: the ER membrane-embedded PERK receptor senses misfolded products in the ER lumen and leads to eIF2α phosphorylation, which transiently reduces protein translation, blocks the import of nascent proteins to the ER and selectively upregulates the translation of specific genes, such as ATF4; ATF4 activates the transcription of cytoprotective genes, including *CHOP*. eIF2α can also be phosphorylated by the kinases GCN2 and PKR. **(B)** HeLa cells were transiently transfected for 24 h with plasmids expressing FLAG-BPLF1, FLAG-BPLF1^{C61A}, FLAG empty vector or treated for 2 h with TPG 1 µM. Cells were lysed with RIPA lysis buffer supplemented with protease inhibitors and western blots were probed with antibodies to p-eIF2α, eIF2α, ATF4, CHOP, FLAG and β-actin. The expression of BPLF1 led to a robust rise of ATF4 and a strong boost of p-eIF2α and CHOP levels, which were significantly abrogated by BPLF1^{C61A}. Western blots from one representative experiment out of five are shown in the figure. Quantification of p-eIF2α, ATF4 and CHOP relative to the empty vector was done using the Image Lab software. The mean ± SD of five experiments is shown. Statistical analysis was performed using Student's *t*-test: ns = $P > 0.05$, * = $P \leq 0.05$.

Inhibition of the ER-RQC and stimulation of the UPR is conserved in β- and γ-herpesviruses

Given that a N-terminal deconjugase domain is highly conserved in the large tegument proteins of all herpesviruses studied to date **(Gastaldello *et al.*, 2010)**, the question that followed was if the effect of BPLF1 on the ER-RQC and the UPR was shared by the homologs encoded by other α-, β- and γ-herpesviruses. To investigate this question, HeLa cells were transiently co-transfected with a S-tagged version of RPL26 (RPL26-S) and FLAG-tagged versions of the N-terminal catalytic domain of the large tegument proteins of different human herpesviruses, which were previously confirmed to be catalytically active **(Figure 2)**: EBV's BPLF1 (FLAG-BPLF1), HSV-1's UL36 (FLAG-UL36), HCMV's UL48 (FLAG-UL48) and KSHV's ORF64 (FLAG-ORF64) **(Figure 6A)**. As control, HeLa cells were also transiently co-transfected with RPL26-S and FLAG-BPLF1^{C61A}. Before lysis, the cells were treated with ANS for 1 h to induce UFMylation. RPL26-S was immunoprecipitated from cell lysates with anti-S agarose beads and the samples were probed with a UFM1-specific antibody. Bands of ~ 28 kDa and ~ 37 kDa likely correspond to mono- and di-UFMylated RPL26, respectively; whether the third band of ~ 46 kDa corresponds to a tri-UFMylated form of RPL26 requires further investigation. Interestingly, while FLAG-BPLF1, FLAG-UL48 and FLAG-ORF64 led to strong decrease of RPL26 UFMylation, the effect was not observed in cells transfected with FLAG-UL36. The reason behind this discrepancy remains to be elucidated, but it is likely to be related with a failure of this specific homologue to interact with one or more partners of the UFM1 conjugation machinery, since UL36 was proven earlier to be catalytically active **(Figure 2)**. Overall, this evidence suggests a conserved activity of the herpesvirus homologues (with exception to UL36) on the impairment of RPL26 UFMylation and, presumably, the ER-RQC pathway. To assess if the herpesvirus

homologues had the same effect as BPLF1 on the modulation of the UPR, HeLa cells were transiently transfected with the FLAG-tagged herpesvirus homologues and the catalytic mutant FLAG-BPLF1^{C61A} **(Figure 6B)**. FLAG-BPLF1 transfection generated a robust increase of the ATF4 levels, which was not observed upon FLAG-BPLF1^{C61A} transfection. Cells transfected with FLAG-UL36 presented similar ATF4 levels to FLAG-BPLF1^{C61A}-transfected cells, suggesting that UL36 catalytic activity fails to upregulate the PERK arm of the UPR. Transfection of FLAG-UL48 and FLAG-ORF64 led to increased amounts of ATF4, establishing these homologues as activators of the pathway.

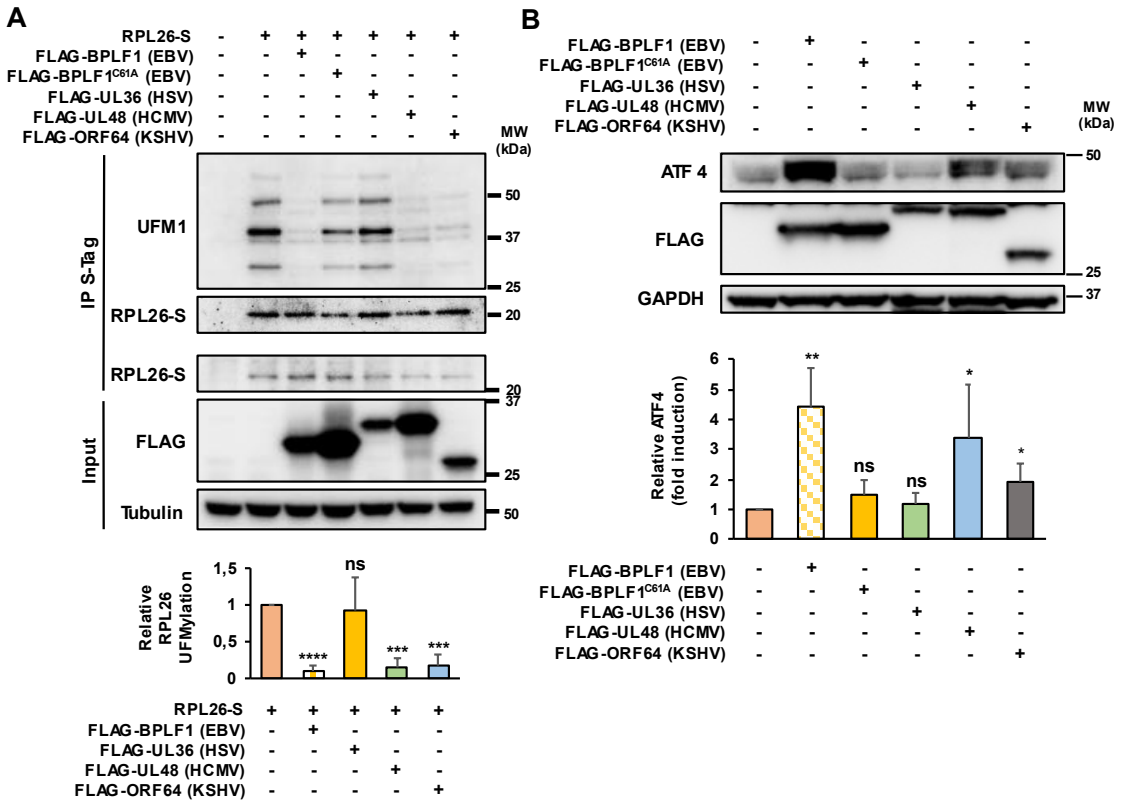

Figure 6. UL48 (HCMV) and ORF64 (KSHV) upregulate the UPR and block the ER-RQC pathway in a similar fashion to BPLF1 (EBV). (A) HeLa cells were transiently co-transfected with plasmids expressing RPL26-S and FLAG-BPLF1, FLAG-BPLF1^{C61A}, FLAG-UL36, FLAG-UL48, FLAG-ORF64 or the FLAG empty vector. Cells were treated with ANS 200 nM for 1 h and lysed with NP40 lysis buffer supplemented with DUB and protease inhibitors. RPL26-S was immunoprecipitated from cell lysates under native conditions in the presence of DUB inhibitors and western blots were probed with antibodies to UFM1, S-tag, FLAG and tubulin. The expression of BPLF1, UL48 and ORF64 impairs the UFMylation of RPL26, while BPLF1^{C61A} and UL36 had a much more moderate effect. Western blots from one representative experiment out of three are shown in the figure. Quantification of RPL26 UFMylation relative to the control transfected with RPL26-S was done using the Image Lab software. The mean ± SD of three experiments is shown. Statistical analysis was performed using Student's *t*-test: ns = $P > 0.05$, *** = $P \leq 0.001$, **** = $P \leq 0.0001$. **(B)** HeLa cells were transiently with plasmids expressing

FLAG-BPLF1, FLAG-BPLF1^{C61A}, FLAG-UL36, FLAG-UL48, FLAG-ORF64 or the FLAG empty vector. Cells were lysed with RIPA lysis buffer supplemented with protease inhibitors and western blots were probed with antibodies to ATF4, FLAG and GAPDH. The expression of BPLF1, UL48 and ORF64 lead to a strong increase of ATF4, while BPLF1^{C61A} and UL36 presented a more modest boost. Western blots from one representative experiment out of two are shown in the figure. Quantification of ATF4 relative to the empty vector was done using the Image Lab software. The mean ± SD of two experiments is shown. Statistical analysis was performed using Student's *t*-test: ns = $P > 0.05$, * = $P \leq 0.05$, ** = $P \leq 0.01$.

Discussion

In accordance with mass spectrometry data that identified the UFM1-specific E3 ligase UFL1 as a potential interactor for BPLF1 **(manuscript in preparation)**, we found that the N-terminal domain of BPLF1 interacts with UFL1 independently of its catalytic activity **(Figure 3)**. Considering the interaction between BPLF1 and UFL1 in *in vitro* experiments and the promiscuous cleavage of Ub and NEDD8 by BPLF1 and other herpesviral DUBs, we wondered if the DUB domain of this class of proteins could also act as a deUFMylase **(Masucci, 2021)**. Indeed, we confirmed that this interaction impaired the conjugation of UFM1 to its own cellular substrate RPL26 and that this effect is dependent on the catalytic activity of BPLF1 **(Figure 4)**. It is noteworthy that during the productive cycle, herpesviruses hijack the cellular translation machinery to allow the production of viral proteins that are subsequently assembled into infectious virions. The herpesviral mRNA contain multiple repeats that can cause ribosomal stalling. Ribosomal stalling during co-translational translocation of viral proteins into the ER would induce activation of the ER-RQC followed by RPL26 UFMylation to enable lysosomal degradation of the nascent polypeptide. Thus, inhibition of the ER-RQC pathway may be beneficial for the virus to maintain the abundance of viral proteins.

Since the impairment of UFMylation was dependent on BPLF1 catalytic activity, we surmised that the BPLF1 N-terminal domain may function as a viral deUFMylase, mimicking the cellular deUFMylase UFSP2. However, our data do not finally prove that BPLF1 is a deUFMylase and alternative explanations should be considered. Two alternative scenarios may explain the capacity of BPLF1 to impair the UFM1 conjugation cascade **(illustrated in Figure 7)**.

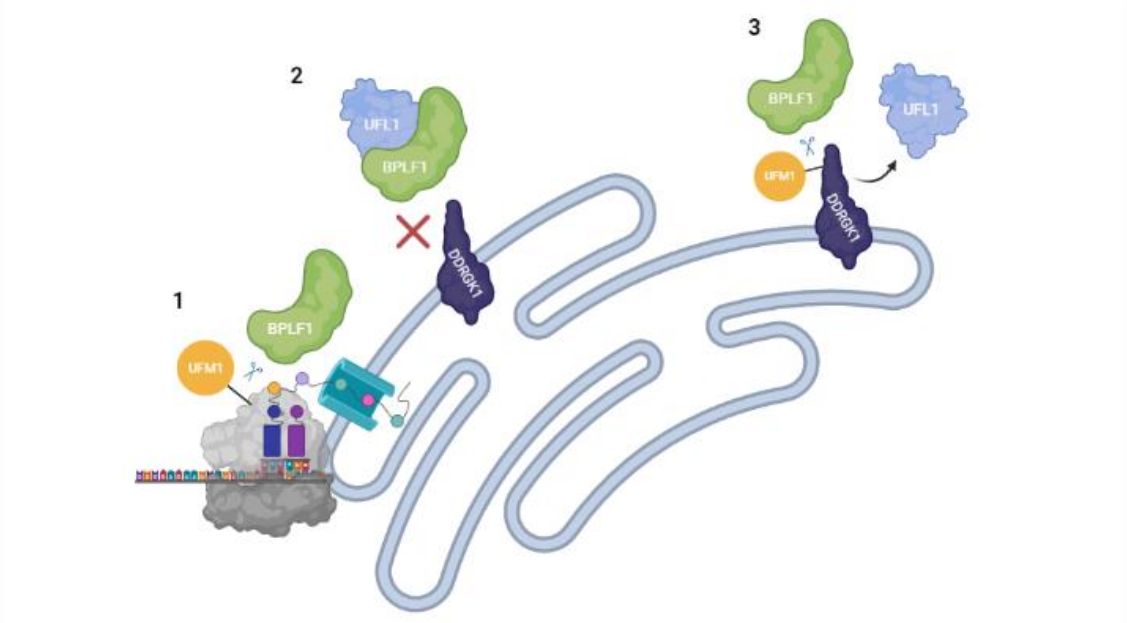

Figure 7. Tripartite model for BPLF1-mediated impairment of UFMylation of cellular substrates. (1) BPLF1 proteolytically cleaves UFM1 from *bona fide* cellular substrates. RPL26 UFMylation induced by ribosome stalling is reversed by BPLF1, which interferes with the activation of the ER-RQC pathway. **(1)** BPLF1 interacts and sequesters the E3 ligase UFL1, preventing its ER localization and the assembly of an active E3 ligase complex. **(2)** BPLF1 deconjugates UFM1 from DDRGK1, thus affecting the stability and the activity of the E3 ligase complex.

The interaction of BPLF1 with UFL1 may interfere with the assembly of the active E3 ligase complex composed by UFL1, DDRGK1 and CDK5RAP3 and/or its localization in the ER membrane **(Figure 7-2)**; alternatively, BPLF1 may selectively interfere with the UFMylation of DDRGK1 **(Figure 7-3)**, which was shown to affect the stability and activity of the E3 ligase complex **(Tatsumi *et al.*, 2010)**.

Here, we detected reduced RPL26 UFMylation in cells transfected with BPLF1 whereas the reduction was not as evident following transfection of BPLF1^{C61A}, suggesting that BPLF1 catalytic activity is implicated in the impairment of RPL26 UFMylation **(Figure 4B)**. Given this evidence, it is not likely that BPLF1 interferes with RPL26 UFMylation by interacting with UFL1 and preventing the localization and assembly of an active E3 ligase complex **(Figure 7, *model 2*)**. Presumably, BPLF1 specifically deUFMylates RPL26 and/or DDRGK1 **(Figure 7, *models 1 and 3*)**. To test this possibility, our group performed *in vitro* experiments where BPLF1 was incubated with RPL26 and the purified components of the UFMylation machinery but failed to conclusively prove that BPLF1 is an active deUFMylase of RPL26 **(not shown)**. However, this possibility cannot be discarded, since RPL26 cannot be UFMylated when isolated from the ribosome. We also tried to test whether BPLF1 may deUFMylate DDRGK1, which would inhibit the assembly of the active ligase, by immunoprecipitating DDRGK1 from cells co-transfected with BPLF1 or BPLF1^{C61A}, but the results that we obtained were also inconclusive. However, the same experiment clearly showed that the interaction of UFL1 with DDRGK1 was reduced in the presence of catalytically active BPLF1 but not in the presence of BPLF1^{C61A} **(not published)**, which supports the hypothesis that BPLF1 may act as a specific deUFMylase of DDRGK1. Ultimately, DDRGK1 deUFMylation affects the stability and activity of the E3 ligase complex, thus impairing RPL26 UFMylation. An additional possibility is that BPLF1 may act upstream of the conjugation of UFM1 to RPL26. For example, BPLF1 may interfere with the initiation of the canonical RQC pathway by deubiquitinating small ribosomal proteins (*e.g.*, RPS2, RPS3, RPS10, RPS20) in the 40S ribosomal subunit. These proteins are ubiquitinated by the E3 ligase ZNF598 after ribosome stalling, which facilitates ribosomal splitting and the exposure of RPL26 to UFMylation. By deubiquitinating small ribosomal proteins, BPLF1 may prevent the activation of both canonical RQC and ER-RQC.

An interesting finding was that the capacity of BPLF1 to modulate the ER-RQC and the UPR responses is shared by some but not all homologs encoded by human herpesviruses. We found that transfection of UL48 (HCMV) and ORF64 (KSHV) resulted in a reduction of UFMylated RPL26 **(Figure 6A)**, suggesting that the DUBs encoded by β- (HCMV) and γ-herpesviruses (KSHV) also interfere with the activation of the ER-RQC. Future research should assess the effect of catalytic mutants of UL48 and ORF64 on RPL26 UFMylation, since our results are not sufficient to confirm that this impairment is dependent on their catalytic activity. On the other hand, transfection of UL36 (HSV-1 and -2) led to a substantially weaker impairment of RPL26 UFMylation, smaller than BPLF1^{C61A} transfection. Since the catalytic activity of UL36 was previously confirmed **(Figure 2)**, these data suggest that UL36 does not prevent RPL26 UFMylation in a scenario of ribosome stalling. However, since the regulation of cellular stress pathways by herpesviruses is a result of a coordinated action of different viral proteins, HSV-1 and HSV-2 may inhibit other branches of the RQC, or other ribosome stress responses, to maintain a constant rate of protein synthesis and promote cell survival. Among them, the integrated stress response (ISR) is activated after ribosome collisions and leads to suppression of protein translation after GCN2-mediated eIF2α phosphorylation and accumulation of ATF4. The upregulation of p-eIF2α and ATF4 triggered by ribosome collisions reveal the intricate cross-talk between the UPR and ribosome stress responses, which led us to the question of whether BPLF1 and its herpesviral counterparts could also exert a more direct effect on the ISR. Nevertheless, the data discussed so far indicate that BPLF1, UL48 and ORF64 impair RPL26 UFMylation, which represents an ingenious strategy of EBV, HCMV and KSHV to overcome ribosome stalling caused by viral protein translation and rescue ER-targeted viral nascent chains from lysosomal degradation.

Independently of the molecular details, the finding that the viral DUBs regulate ribosomal and ER stress responses has interesting implication for the biology of herpesvirus infection.

Activation of the productive cycle is associated with a massive influx of misfolded viral products into the ER lumen. This may overwhelm the folding capacity of the ER and cause ER stress, triggering the activation of the UPR, which, if uncontrolled, may lead the cell to apoptosis. In order to prevent apoptosis and to create a permissive environment for viral protein synthesis, herpesviruses use multiple strategies to modulate different branches of the UPR in their favour **(Johnston & McCormick, 2019)**. For example, herpesviruses may promote the synthesis of chaperone proteins and expansion of the ER network to support production and folding of viral proteins. Most importantly, herpesviruses strongly inhibit bulk cellular protein synthesis. Regulation of the UPR is coordinated by different herpesviral proteins and the type of modulation may vary depending on the phase of the productive cycle. For example, *BRLF1* and *BZLF1*, two essential EBV's immediate early viral genes, and the oncogene *LMP1* were found to be transcriptionally activated by XBP1 **(Bhende *et al.*, 2007; Hsiao *et al.*, 2009)**. Also,

expression of *LMP1* activates PERK, resulting in eIF2α phosphorylation and accumulation of ATF4. Although eIF2α phosphorylation presumably leads to attenuation of protein synthesis, ATF4 recognizes the *LMP1* promoter and can, thus, upregulate *LMP1* transcription **(Lee *et al.*, 2008)**. Even though the transcription of EBV genes is promoted by ATF4, how can translation of EBV proteins proceed if eIF2α is phosphorylated and bulk protein synthesis is suppressed? A plausible explanation may rely on upstream open reading frames (uORFs) contained in 5' untranslated regions (5'UTRs) of EBV mRNAs. uORFs are short nucleotide sequences encoded upstream of a main ORF that regulate the translation of the latter. Stress genes are acknowledged to be regulated via this mechanism. ATF4, for instance, is known to be regulated by two uORFs: in the absence of stress, uORF1 is efficiently translated and ribosome scanning resumes at uORF2, overlapping the main ORF and repressing the expression of ATF4; however, under stress conditions, high levels of p-eIF2α are thought to induce *leaky scanning* of the ATF4 5'UTR region, resulting in bypass of uORF2 translation and translation reinitiation at the main ORF. EBV and other herpesviruses were also found to encode uORFs, which operate as *speed bumps* for the translation of main ORFs, even under p-eIF2α repression **(Glaunsinger, 2015; Watanabe *et al.*, 2015)**. By promoting eIF2α phosphorylation (which downregulates bulk protein translation but upregulates the translation of EBV mRNAs with upstream uORFs) and by inducing ATF4 accumulation (which promotes the expression of cytoprotective genes and EBV genes that are ATF4-responsive), EBV safeguards a constant production of viral proteins and promotes cell survival, which are two pivotal conditions for the success of the productive cycle. In accordance with our results, BPLF1 transfection leads to an increase of eIF2α phosphorylation, together with a strong accumulation of ATF4 and CHOP **(Figure 5B)**. On the other hand, BPLF1^{C61A} transfection led to a smaller upregulation, indicating that BPLF1 catalytic activity is involved in the accumulation of p-eIF2α, ATF4 and CHOP. eIF2α can be phosphorylated by four kinases in a stress-dependent manner: PERK, PKR, GCN2 and HRI (heme-regulated inhibitor) **(Donnelly *et al.*, 2013)**. To investigate the mechanism by which BPLF1 upregulates eIF2α phosphorylation, we conducted experiments where cells transfected with BPLF1 were treated with ISRIB (an inhibitor of eIF2α phosphorylation), a PKR inhibitor or a PERK inhibitor. However, our results were not conclusive and we did not test inhibitors of GCN2 and HRI **(not shown)**. Although we could not identify a definitive mechanism by which BPLF1 catalytic activity induces this branch of the UPR, a plausible explanation may rely on the accumulation of viral misfolded products in the ER lumen (which activate the PERK receptor) after the deubiquitination of viral misfolded products that were targeted for proteasomal degradation. Another possible answer consists of the activation of GCN2 (which leads to eIF2α phosphorylation) by ribosome collisions that can be caused by ER-RQC failure after BPLF1 impairment of RPL26 UFMylation.

Other members of the *Herpesviridae* family were previously demonstrated to modulate the UPR in their favour during the productive cycle. In a similar fashion to

EBV, regulation of the UPR by herpesviruses is orchestrated by the simultaneous activity of different viral proteins **(Johnston & McCormick, 2019)**. Here, we confirm that the DUBs encoded in the large tegument proteins of β- (HCMV) and γ-herpesviruses (KSHV) induce accumulation of ATF4. The rationale behind the upregulation of ATF4 by UL48 and ORF64 may be similar to BPLF1. Surprisingly, expression of the DUB of two α-herpesviruses (HSV-1 and -2) failed to upregulate ATF4, leading to similar levels to the ones caused by $BPLF1^{C61A}$ transfection. This result suggests that the catalytic core of UL36 may not be involved in the accumulation of ATF4. Although the reason behind this discrepancy remains elusive, several studies revealed that, in contrast to β- and γ-herpesviruses, HSV-1 specifically prevents the transcription of ATF4 and CHOP, even if PERK becomes activated during viral infection. Possibly, this selective regulation avoids deleterious cellular responses to HSV-1 that are mediated by ATF4, such as autophagy.

Overall, the present study validates the DUBs encoded in the N-terminal region of the large tegument proteins of herpesviruses as strong modulators of cellular responses to ER and ribosomal stresses induced by activation of the productive cycle. Although the molecular mechanisms underneath the modulation of the UPR and the ER-RQC by these herpesviral DUBs are still unknown, the findings presented in this study pave the road for future research on remaining questions. For example, the molecular events that culminate in the accumulation of p-eIF2α, ATF4 and CHOP occur upstream (*e.g.*, accumulation of misfolded proteins that can activate the PERK receptor) or independently of (*e.g.*, activation of PKR or GCN2 resulting in eIF2α phosphorylation) the PERK sensor remain to be determined. Finding a definitive answer to this question may be difficult, since the cross-talk between UPR branches also opens the possibility of a modulatory effect of these herpesviral DUBs on the IRE1α or ATF6α pathways. On a different note, it would be relevant to determine the actual molecular mechanism for the impairment of RPL26 UFMylation by these viral DUBs and investigating whether they can also modulate the canonical RQC pathway. Ultimately, a better understanding on these regulatory mechanisms would be beneficial for the design of specific inhibitors of these herpesviral DUBs, which could improve the therapeutic window for immunocompromised individuals.

Materials & Methods

Cell lines and transfection

HeLa cells (ATCC RR-B51S) were cultured in 75 cm^2 culture flasks with 15 mL Dulbecco's minimal essential medium (DMEM) supplemented with 10% FBS and 10 µg/mL ciprofloxacin and grown in a 37 ºC incubator with 5% CO_2. Before plating, cells were washed once with phosphate buffer saline (PBS) and incubated in the incubator with 3 mL 1x trypsin-EDTA (diluted in PBS) until being detached. Trypsin-EDTA was neutralized with 12 mL DMEM and the cells were transferred to a tube. After counting, cells were seeded in 6-well cell culture plates or 100 mm x 20 mm cell culture dishes and cultured until reaching 70-90% confluency. Cells were transiently transfected for 24 or 48 h with plasmids expressing tagged proteins using Lipofectamine 3000 Transfection Kit and Opti-MEM reduced serum medium (1X) using the Opti-MEM recommended by the manufacturer. Cells seeded in 6-well plates were transfected with 2 µg DNA, while cells plated in dishes were transfected with 10 µg DNA. A 3:1:3 ratio of Lipofectamine 3000 (µL) : DNA (µg) : p3000 reagent was used, based on previous optimization of the protocol recommended by the manufacturer.

Western blots

Cells seeded in a 6-well plate were washed once with DPBS and placed in the incubator with 250 µL 1X trypsin-EDTA (diluted in DPBS) until being detached. Trypsin-EDTA was neutralized with 1 mL DMEM and cells were transferred to tubes and kept on ice. Cells were centrifuged at 2000 x g at 4 ºC for 5 min and the supernatants were discarded. Next, cells were lysed in 100 µL RIPA lysis buffer (50 mM Tris-HCl pH 7.4, 150 mM NaCl, 0.5% sodium deoxycholate, 0.1% SDS, 1% Triton X-100) or NP40 lysis buffer (150 mM NaCl, 50 mM Tris-HCl pH 7.6, 5 mM $MgCl_2$, 1 mM EDTA, 1% IGEPAL, 5% glycerol) supplemented with 1X complete protease inhibitor cocktail and, if necessary, DUB inhibitors (20 mM *N*-ethylmaleimide (NEM) and 20 mM iodoacetamide) for 30 min on ice. Cell lysates were centrifuged at 13 000 x g at 4 ºC for 30 min and supernatants were transferred to new tubes. Protein concentration was calculated using a Lowry protein assay and equalized by adding lysis buffer. Then, 25 µL 1x LDS sample buffer and 10 µL 1x sample reducing agent were added to 65 µL cell lysates, followed by boiling for 5 min at 100 ºC. The lysates were fractionated in acrylamide gels immersed in 1X MOPS running buffer. Transfer to PVDF membranes (previously activated with pure methanol for 1 min and briefly washed with water) was performed in transfer buffer (25.6 mM Trizma base, 186 mM glycine, 20% methanol) for 90 min with constant current (0.28 A). The blots were blocked in blocking buffer (TBS-T (1X TBS, 0.1% Tween 20), 5% non-fat milk) for 1 h with shaking. The membranes

were incubated with the primary antibodies diluted in blocking buffer for 1 h or overnight at 4 ºC with shaking, followed by 5 washes with TBS-T during 30 min with shaking. The blots were incubated for 1 h with shaking with the appropriate horseradish peroxidase-conjugated secondary antibodies diluted in blocking buffer, followed by 5 washes with TBS-T during 30 min with shaking. The immunocomplexes were visualized by enhanced chemiluminescence using the Bio-Rad ChemiDoc™ MP imaging system.

DUB functional assay

Cells seeded in a 6-well plate were lysed in 100 µL NP40 lysis buffer supplemented with 1X complete protease inhibitor cocktail and the protocol described in the **Western blots** section was followed. After equalizing protein concentrations, cell lysates with 10 µg protein were incubated with 1 µM HA-Ub-VS probe and 1X reaction buffer (50 mM Tris-HCl pH 7.4, 5 mM $MgCl_2$, 1 mM DTT, 0.5% sucrose). ddH_2O was added to reach a final volume of 30 µL. Controls without the HA-Ub-VS probe were also included, adding the corresponding volume of ddH_2O instead of the probe. The mixture was homogenised with a pipette and incubated at 37 ºC for 1 h. The reaction was stopped by adding 10 µL 4X LDS sample buffer to the tubes and samples were fractionated in acrylamide gels, as described in the **Western blots** section.

Immunoprecipitation (IP) and pull-down assays

Cells plated in dishes were washed twice with DPBS and detached using cell scrappers after 24 or 48 h of transfection. Afterwards, cells were lysed in 1 mL NP40 lysis buffer (150 mM NaCl, 50 mM Tris-HCl pH 7.6, 5 mM $MgCl_2$, 1 mM EDTA, 1% IGEPAL, 5% glycerol) supplemented with 1X protease inhibitor cocktail, 20 mM NEM and 20 mM iodoacetamide for 30 min on ice. In alternative to the incubation on ice, cells were passed through a slim needle coupled to a syringe. For IPs under denaturing conditions **(Figures 3B and 5A)**, the lysis buffer was supplemented with 1% SDS followed by dilution to 0.1% SDS before IP. Cell lysates were centrifuged at 13 000 x g at 4 ºC for 30 min and the supernatants were transferred to new tubes. Protein concentration was determined and equalized using the method described in the **Western blots** section. Input samples were prepared according to the protocol described in the **Western blots** section.

For BPLF1/BPLF1^{C61A} co-IP and RPL26 IP, 50 µL anti-FLAG, anti-c-Myc or anti-S packed affinity gels were washed with 1 mL lysis buffer for 5 min at 4 ºC with rotation and the lysis buffer was discarded after centrifuging for 5 min at 1 500 x g at 4 ºC. Next, equal volumes of cell lysates were added to the beads and incubated for 3 h at 4 ºC with rotation (or left overnight in the same conditions). After this step, beads and cell lysates were centrifuged at 1 500 x g for 5 min at 4 ºC and supernatants were discarded. The beads were washed with 1 mL lysis buffer for 5 min at 4 ºC with rotation,

centrifuged at 1 500 x g for 5 min at 4 ºC and supernatants were discarded. This washing step was repeated 4 times, before boiling the beads in 20 µL 2X loading buffer, 4 µL 1X sample reducing agent and 16 µL lysis buffer for 10 min at 100 ºC. Samples were centrifuged at 1 500 x g for 2 min and the supernatants were stored in new tubes.

For UFL1 IP, 40 µL protein-G coupled sepharose beads were washed in 1 mL lysis buffer for 5 min at 4 ºC with rotation, followed by centrifugation at 1 500 x g for 5 min at 4 ºC and discard of the supernatants. Then, cell lysates were added to the beads and incubated for 30 min at 4 ºC with rotation, centrifuged at 1 500 x g for 5 min at 4 ºC and supernatants were transferred to new tubes (named **pre-clearance step**). After protein quantification and equalization (see **Western blots** section), an anti-UFL1 specific antibody was added to the pre-cleared cell lysates (or, in the case of the control, an IgG antibody) and incubated at 4 ºC for 2 h with rotation. The protein-antibody complexes were captured with 50 µL sepharose beads (previously washed, *see above*) by incubation with rotation at 4 ºC for 1 h. The beads were washed and the samples were prepared similarly to the protocol described for BPLF1/BPLF1^{C61A} co-IP and RPL26 IP (*see above*).

Statistical analysis

Statistical analysis was performed using Student's *t*-test on Microsoft Office Excel software.

Table 1. List of materials used during this project.

Cell culture and transfection		
Materials	**Sources**	**Identifiers**
6-well culture plates	Corning, Corning, NY, USA	Cat# 3506
75 cm^2 culture flasks	TPP, Trasadingen, CH	Cat# 90076
100 mm x 20 mm cell culture dishes	Corning	Cat# 430167
Centrifuge 5417R	Eppendorf, Hamburg, DE	Not available
Reagents	**Sources**	**Identifiers**
0.5% Trypsin-EDTA (10X)	Gibco, Waltham, MA, USA	Cat# 15400-054

Ciprofloxacin (CPX)	Sigma-Aldrich, St. Louis, MO, USA	Cat# 17850	
Dulbecco's minimal essential medium (DMEM)	Sigma-Aldrich	Cat# D6429	
Dulbecco's phosphate buffered saline (DPBS)	Sigma-Aldrich	Cat #D8537	
Fetal bovine serum (FBS)	Gibco	Cat# 16000044	
Lipofectamine® 3000 Transfection Kit	Invitrogen, Waltham, MA, USA	Cat# L3000-015	
Opti-MEM™ reduced serum medium	Gibco	Cat# 31985070	
Plasmids	**Sources**	**Identifiers**	
pCMV10-3xFLAG	Previously described in Gastaldello *et al.* (2010) and in Gastaldello *et al.* (2012)		
pCMV10-3xFLAG-BPLF1 (1-235 aa)			
pCMV10-3xFLAG-BPLF1^{C61A}(1-235 aa)			
pCMV10-3xFLAG-ORF64 (1-265 aa)			
pCMV3-RPL26-Myc	Sino Biological, Eschborn, DE	Cat# HG16834-CM	
pCMV10-3xFLAG-UL36 (1-293 aa)	Previously described in Ylä-Antilla & Masucci (2021)		
pCMV10-3xFLAG-UL48 (1-263)			
Western blots, immunoprecipitation (IP) and pull-down assays, DUB functional assay			
Antibodies & beads	**Sources**	**Dilutions**	**Identifiers**
Rabbit monoclonal anti-ATF4 (D4B8)	Cell Signaling Technology, Danvers, MA, USA	1:1000	Cat# 11815
Mouse monoclonal anti-β-actin clone AC-15	Sigma-Aldrich	1:5000	Cat# A5441

Mouse monoclonal anti-CHOP (L63F7)	Cell Signaling Technology	1:1000	Cat# 2895
Mouse monoclonal anti-eIF2α (L57A5)	Cell Signaling Technology	1:1000	Cat# 2103
Mouse monoclonal anti-FLAG	Sigma-Aldrich	1:10000	Cat# F3165
Mouse monoclonal anti-GAPDH	Millipore, Burlington, MA, USA	1:10000	Cat# CB1001
Rabbit monoclonal anti-Myc tag	Cell Signaling Technology	1:1000	Cat# 2278
Rabbit anti-phospho-eIF2α (Ser51) (D9G8) XP	Cell Signaling Technology	1:1000	Cat# 3398
Mouse monoclonal anti-S tag	Millipore	1:3000	Cat# 71549-3
Mouse monoclonal anti-tubulin	Millipore	1:2000	Cat# CP06
Rabbit polyclonal anti-UFL1	Bethyl Laboratories, Montgomery, TX, USA	1:5000 1:87 (cross-IP)	Cat# A303-456A
Rabbit monoclonal anti-UFM1	Abcam, Cambridge, GB	1:3000	Cat# ab109305
Rabbit monoclonal IgG	Abcam	1:870	Cat# ab172730
Rabbit anti-FLAG® M2 affinity gel	Sigma-Aldrich	~ 1:20	Cat# A2220
Rabbit anti-c-Myc agarose affinity gel	Sigma-Aldrich	~ 1:20	Cat# A7470
S-protein agarose	Millipore	~ 1:20	Cat# 69704
GammaBind™ Plus Sepharose™	Cytiva, Marlborough, MA, USA	1:10.9 (washing step) 1:8.7 (IP)	Cat# 17088601
Anti-mouse IgG, horseradish peroxidase-linked whole antibody	Cytiva	1:10000	Cat# NXA931

Anti-rabbit IgG, horseradish peroxidase-linked whole antibody	Cytiva	1:10000	Cat# NA934
Recombinant Human HA-Ubiquitin Vinyl Sulfone Protein	R&D Systems, Minneapolis, MN, USA	1:30000	Cat#U-212-025
Materials	**Sources**	**Identifiers**	
Acrylamide Bis-Tris 4-12% gradient gel	Invitrogen	Cat# NP0321BOX/NP0323BOX	
ChemiDoc™ MP imaging system	Bio-Rad, Hercules, CA, USA	Cat# 12003154	
Immobilon®-P membrane, PVDF, 0.45 µm, 8.5 cm x 10 m roll	Millipore	Cat# IPVH85R	
Microlance hypodermic needle 27G x 3/4"	Becton Dickinson, Huesca, ES	Cat# 302200	
PowerPac 200	Bio-Rad	Not available	
Reagents	**Sources**	**Identifiers**	
AccuGENE™ 1 M Tris-HCl Buffer	Lonza, Rockland, ME, USA	Cat# 51237	
Anisomycin (ANS)	Sigma-Aldrich	Cat# A5862	
cOmplete™ protease inhibitor cocktail	Roche, Basel, CH	Cat# 04693116001	
DC™ protein assay kit II	Bio-Rad	Cat# 5000112	
DL-Dithiothreitol (DTT)	Sigma-Aldrich	Cat# D0632	
Ethylenediaminetetraacetic acid (EDTA) solution	Sigma-Aldrich	Cat# E8008	
Glycerol	Sigma-Aldrich	Cat# 49781	
Glycine	Fisher Scientific, Waltham, MA, USA	Cat# 10070150	
IGEPAL® CA-630 (NP40)	Sigma-Aldrich	Cat# I3021	
Iodoacetamide	Sigma-Aldrich	Cat# I1149	

Magnesium chloride hexahydrate ($MgCl_2$)	SAFC, St. Louis, MO, USA	Cat# 172571
Methanol	Fisher Chemical, Waltham, MA, USA	Cat# 11976961
N-ethylmaleimide (NEM)	Sigma-Aldrich	Cat# E1271
Nonfat dried milk powder	PanReac/AppliChem, Glenview, IL, USA	Cat# A0830
NuPAGE™ LDS sample buffer (4X)	Invitrogen	Cat# NP0008
NuPAGE™ MOPS SDS running buffer (20X)	Invitrogen	Cat# NP000102
NuPAGE™ sample reducing agent (10X)	Invitrogen	Cat# NP0009
Sodium chloride (NaCl)	Fisher Chemical	Cat# 10428420
Sodium deoxycholate	Sigma-Aldrich	Cat# D6750
Sodium dodecyl sulphate (SDS)	Supelco, St. Louis, MO, USA	Cat# 74255
Sucrose	Duchefa Biochemie, Haarlem, NL	Cat# S0809
SuperSignal™ West Pico PLUS chemiluminescent substrate	Thermo Scientific, Waltham, MA, USA	Cat# 34580
Thapsigargin (TPG)	Sigma-Aldrich	Cat# T9033
Tris buffered saline (TBS) (10X, pH 7.4)	Fisher Scientific	Cat# BP2471-1
Triton™ X-100	Sigma-Aldrich	Cat# T9284
Trizma® base	Sigma-Aldrich	Cat# 93349
Tween® 20	Sigma-Aldrich	Cat# P9416

Acknowledgements

First, I would like to thank Maria for giving me the opportunity to do my Master's thesis internship in her laboratory and also for all the support and kindness during my stay in Stockholm. I am sure that this experience will have a great impact on my future as a researcher and that Maria's expertise provided me tools that will be absolutely critical for my career. I would also like to thank Jiangnan for being always helpful and for all the practical skills I got from him. And, of course, I could not forget Carlos, Noemi and Paco for being always free to help. Finally, I would like to thank all the friends I made during this year in Stockholm. It only felt so short because of you and you shan't be forgotten (insert candle emoji). At last, my friends and family in Portugal. You made me realize what the word *saudade* truly means.

References

1. Babcock, G. J., Decker, L. L., Volk, M., & Thorley-Lawson, D. A. (1998). EBV persistence in memory B cells in vivo. *Immunity*, *9*(3), 395–404. https://doi.org/10.1016/s1074-7613(00)80622-6
2. Bhende, P. M., Dickerson, S. J., Sun, X., Feng, W. H., & Kenney, S. C. (2007). X-box-binding protein 1 activates lytic Epstein-Barr virus gene expression in combination with protein kinase D. *Journal of virology*, *81*(14), 7363–7370. https://doi.org/10.1128/JVI.00154-07
3. Cai, Y., Pi, W., Sivaprakasam, S., Zhu, X., Zhang, M., Chen, J., Makala, L., Lu, C., Wu, J., Teng, Y., Pace, B., Tuan, D., Singh, N., & Li, H. (2015). UFBP1, a Key Component of the Ufm1 Conjugation System, Is Essential for Ufmylation-Mediated Regulation of Erythroid Development. *PLoS genetics*, *11*(11), e1005643. https://doi.org/10.1371/journal.pgen.1005643
4. Cohen J. I. (2020). Herpesvirus latency. *The Journal of clinical investigation*, 130(7), 3361–3369. https://doi.org/10.1172/JCI136225
5. de-Thé, G., Day, N. E., Geser, A., Lavoué, M. F., Ho, J. H., Simons, M. J., Sohier, R., Tukei, P., Vonka, V., & Zavadova, H. (1975). Sero-epidemiology of the Epstein-Barr virus: preliminary analysis of an international study - a review. *IARC scientific publications*, (11 Pt 2), 3–16.
6. Donnelly, N., Gorman, A. M., Gupta, S., & Samali, A. (2013). The eIF2α kinases: their structures and functions. *Cellular and molecular life sciences : CMLS*, *70*(19), 3493–3511. https://doi.org/10.1007/s00018-012-1252-6
7. Dyson, O. F., Pagano, J. S., & Whitehurst, C. B. (2017). The Translesion Polymerase Pol η Is Required for Efficient Epstein-Barr Virus Infectivity and Is Regulated by the Viral Deubiquitinating Enzyme BPLF1. *Journal of virology*, *91*(19), e00600-17. https://doi.org/10.1128/JVI.00600-17
8. Garreau de Loubresse, N., Prokhorova, I., Holtkamp, W., Rodnina, M. V., Yusupova, G., & Yusupov, M. (2014). Structural basis for the inhibition of the eukaryotic ribosome. *Nature*, *513*(7519), 517–522. https://doi.org/10.1038/nature13737
9. Garshott, D. M., Sundaramoorthy, E., Leonard, M., & Bennett, E. J. (2020). Distinct regulatory ribosomal ubiquitylation events are reversible and hierarchically organized. *eLife*, *9*, e54023. https://doi.org/10.7554/eLife.54023
10. Gastaldello, S., Hildebrand, S., Faridani, O., Callegari, S., Palmkvist, M., Di Guglielmo, C., & Masucci, M. G. (2010). A deneddylase encoded by Epstein-Barr virus promotes viral DNA replication by regulating the activity of cullin-RING ligases. *Nature cell biology*, *12*(4), 351–361. https://doi.org/10.1038/ncb2035
11. Gastaldello, S., Callegari, S., Coppotelli, G., Hildebrand, S., Song, M., & Masucci, M. G. (2012). Herpes virus deneddylases interrupt the cullin-RING ligase

neddylation cycle by inhibiting the binding of CAND1. *Journal of molecular cell biology*, *4*(4), 242–251. https://doi.org/10.1093/jmcb/mjs012

12. Gerakis, Y., Quintero, M., Li, H., & Hetz, C. (2019). The UFMylation System in Proteostasis and Beyond. *Trends in cell biology*, *29*(12), 974–986. https://doi.org/10.1016/j.tcb.2019.09.005

13. Glaunsinger B. A. (2015). Modulation of the Translational Landscape During Herpesvirus Infection. *Annual review of virology*, *2*(1), 311–333. https://doi.org/10.1146/annurev-virology-100114-054839

14. Gupta, S., Ylä-Anttila, P., Callegari, S., Tsai, M. H., Delecluse, H. J., & Masucci, M. G. (2018). Herpesvirus deconjugases inhibit the IFN response by promoting TRIM25 autoubiquitination and functional inactivation of the RIG-I signalosome. *PLoS pathogens*, *14*(1), e1006852. https://doi.org/10.1371/journal.ppat.1006852

15. Gupta, S., Ylä-Anttila, P., Sandalova, T., Sun, R., Achour, A., & Masucci, M. G. (2019). 14-3-3 scaffold proteins mediate the inactivation of trim25 and inhibition of the type I interferon response by herpesvirus deconjugases. *PLoS pathogens*, *15*(11), e1008146. https://doi.org/10.1371/journal.ppat.1008146

16. Habisov, S., Huber, J., Ichimura, Y., Akutsu, M., Rogova, N., Loehr, F., McEwan, D. G., Johansen, T., Dikic, I., Doetsch, V., Komatsu, M., Rogov, V. V., & Kirkin, V. (2016). Structural and Functional Analysis of a Novel Interaction Motif within UFM1-activating Enzyme 5 (UBA5) Required for Binding to Ubiquitin-like Proteins and Ufmylation. *The Journal of biological chemistry*, *291*(17), 9025–9041. https://doi.org/10.1074/jbc.M116.715474

17. Hammerschmidt, W., & Sugden, B. (2013). Replication of Epstein-Barr viral DNA. *Cold Spring Harbor perspectives in biology*, *5*(1), a013029. https://doi.org/10.1101/cshperspect.a013029

18. Hetz, C., Zhang, K., & Kaufman, R. J. (2020). Mechanisms, regulation and functions of the unfolded protein response. *Nature reviews. Molecular cell biology*, *21*(8), 421–438. https://doi.org/10.1038/s41580-020-0250-z

19. Hochstrasser M. (2009). Origin and function of ubiquitin-like proteins. *Nature*, *458*(7237), 422–429. https://doi.org/10.1038/nature07958

20. Houen, G., Trier, N. H., & Frederiksen, J. L. (2020). Epstein-Barr Virus and Multiple Sclerosis. *Frontiers in immunology*, *11*, 587078. https://doi.org/10.3389/fimmu.2020.587078

21. Hsiao, J. R., Chang, K. C., Chen, C. W., Wu, S. Y., Su, I. J., Hsu, M. C., Jin, Y. T., Tsai, S. T., Takada, K., & Chang, Y. (2009). Endoplasmic reticulum stress triggers XBP-1-mediated up-regulation of an EBV oncoprotein in nasopharyngeal carcinoma. *Cancer research*, *69*(10), 4461–4467. https://doi.org/10.1158/0008-5472.CAN-09-0277

22. Hurley, J. H., Lee, S., & Prag, G. (2006). Ubiquitin-binding domains. *The Biochemical journal*, *399*(3), 361–372. https://doi.org/10.1042/BJ20061138

23. Ishimura, R., Obata, M., Kageyama, S., Daniel, J., Tanaka, K., & Komatsu, M. (2017). A novel approach to assess the ubiquitin-fold modifier 1-system in cells. *FEBS letters*, *591*(1), 196–204. https://doi.org/10.1002/1873-3468.12518

24. Joazeiro C. (2019). Mechanisms and functions of ribosome-associated protein quality control. *Nature reviews. Molecular cell biology*, *20*(6), 368–383. https://doi.org/10.1038/s41580-019-0118-2

25. Johnston, B. P., & McCormick, C. (2019). Herpesviruses and the Unfolded Protein Response. *Viruses*, *12*(1), 17. https://doi.org/10.3390/v12010017

26. Kerscher, O., Felberbaum, R., & Hochstrasser, M. (2006). Modification of proteins by ubiquitin and ubiquitin-like proteins. *Annual review of cell and developmental biology*, *22*, 159–180. https://doi.org/10.1146/annurev.cellbio.22.010605.093503

27. Komatsu, M., Chiba, T., Tatsumi, K., Iemura, S., Tanida, I., Okazaki, N., Ueno, T., Kominami, E., Natsume, T., & Tanaka, K. (2004). A novel protein-conjugating system for Ufm1, a ubiquitin-fold modifier. *The EMBO journal*, *23*(9), 1977–1986. https://doi.org/10.1038/sj.emboj.7600205

28. Kumar, R., Whitehurst, C. B., & Pagano, J. S. (2014). The Rad6/18 ubiquitin complex interacts with the Epstein-Barr virus deubiquitinating enzyme, BPLF1, and contributes to virus infectivity. *Journal of virology*, *88*(11), 6411–6422. https://doi.org/10.1128/JVI.00536-14

29. Lee, D. Y., & Sugden, B. (2008). The LMP1 oncogene of EBV activates PERK and the unfolded protein response to drive its own synthesis. *Blood*, *111*(4), 2280–2289. https://doi.org/10.1182/blood-2007-07-100032

30. Lemaire, K., Moura, R. F., Granvik, M., Igoillo-Esteve, M., Hohmeier, H. E., Hendrickx, N., Newgard, C. B., Waelkens, E., Cnop, M., & Schuit, F. (2011). Ubiquitin fold modifier 1 (UFM1) and its target UFBP1 protect pancreatic beta cells from ER stress-induced apoptosis. *PloS one*, *6*(4), e18517. https://doi.org/10.1371/journal.pone.0018517

31. Li, J., Nagy, N., Liu, J., Gupta, S., Frisan, T., Hennig, T., Cameron, D. P., Baranello, L., & Masucci, M. G. (2021). The Epstein-Barr virus deubiquitinating enzyme BPLF1 regulates the activity of topoisomerase II during productive infection. *PLoS pathogens*, *17*(9), e1009954. https://doi.org/10.1371/journal.ppat.1009954

32. Liang, J. R., Lingeman, E., Luong, T., Ahmed, S., Muhar, M., Nguyen, T., Olzmann, J. A., & Corn, J. E. (2020). A Genome-wide ER-phagy Screen Highlights Key Roles of Mitochondrial Metabolism and ER-Resident UFMylation. *Cell*, *180*(6), 1160–1177.e20. https://doi.org/10.1016/j.cell.2020.02.017

33. Lindner, P., Christensen, S. B., Nissen, P., Møller, J. V., & Engedal, N. (2020). Cell death induced by the ER stressor thapsigargin involves death receptor 5, a non-autophagic function of MAP1LC3B, and distinct contributions from unfolded protein response components. *Cell communication and signaling : CCS*, *18*(1), 12. https://doi.org/10.1186/s12964-019-0499-z

34. Liu, J., Guan, D., Dong, M., Yang, J., Wei, H., Liang, Q., Song, L., Xu, L., Bai, J., Liu, C., Mao, J., Zhang, Q., Zhou, J., Wu, X., Wang, M., & Cong, Y. S. (2020).

UFMylation maintains tumour suppressor p53 stability by antagonizing its ubiquitination. *Nature cell biology*, *22*(9), 1056–1063. https://doi.org/10.1038/s41556-020-0559-z

35. Masucci M. G. (2021). Herpesvirus ubiquitin deconjugases. *Seminars in cell & developmental biology*, S1084-9521(21)00274-3. Advance online publication. https://doi.org/10.1016/j.semcdb.2021.10.011

36. Meyer, C., Garzia, A., Morozov, P., Molina, H., & Tuschl, T. (2020). The G3BP1-Family-USP10 Deubiquitinase Complex Rescues Ubiquitinated 40S Subunits of Ribosomes Stalled in Translation from Lysosomal Degradation. Molecular cell, *77*(6), 1193–1205.e5. https://doi.org/10.1016/j.molcel.2019.12.024

37. Padala, P., Oweis, W., Mashahreh, B., Soudah, N., Cohen-Kfir, E., Todd, E. A., Berndsen, C. E., & Wiener, R. (2017). Novel insights into the interaction of UBA5 with UFM1 via a UFM1-interacting sequence. *Scientific reports*, *7*(1), 508. https://doi.org/10.1038/s41598-017-00610-0

38. Park, J., Park, J., Lee, J., & Lim, C. (2021). The trinity of ribosome-associated quality control and stress signaling for proteostasis and neuronal physiology. *BMB reports*, *54*(9), 439–450. https://doi.org/10.5483/BMBRep.2021.54.9.097

39. Pisareva, V. P., Skabkin, M. A., Hellen, C. U., Pestova, T. V., & Pisarev, A. V. (2011). Dissociation by Pelota, Hbs1 and ABCE1 of mammalian vacant 80S ribosomes and stalled elongation complexes. *The EMBO journal*, *30*(9), 1804–1817. https://doi.org/10.1038/emboj.2011.93

40. Saito, S., Murata, T., Kanda, T., Isomura, H., Narita, Y., Sugimoto, A., Kawashima, D., & Tsurumi, T. (2013). Epstein-Barr virus deubiquitinase downregulates TRAF6-mediated NF-κB signaling during productive replication. *Journal of virology*, *87*(7), 4060–4070. https://doi.org/10.1128/JVI.02020-12

41. Schlieker, C., Korbel, G. A., Kattenhorn, L. M., & Ploegh, H. L. (2005). A deubiquitinating activity is conserved in the large tegument protein of the herpesviridae. *Journal of virology*, *79*(24), 15582–15585. https://doi.org/10.1128/JVI.79.24.15582-15585.2005

42. Shannon-Lowe, C., & Rickinson, A. (2019). The Global Landscape of EBV-Associated Tumors. *Frontiers in oncology*, *9*, 713. https://doi.org/10.3389/fonc.2019.00713

43. Tatsumi, K., Sou, Y. S., Tada, N., Nakamura, E., Iemura, S., Natsume, T., Kang, S. H., Chung, C. H., Kasahara, M., Kominami, E., Yamamoto, M., Tanaka, K., & Komatsu, M. (2010). A novel type of E3 ligase for the Ufm1 conjugation system. *The Journal of biological chemistry*, *285*(8), 5417–5427. https://doi.org/10.1074/jbc.M109.036814

44. van der Veen, A. G., & Ploegh, H. L. (2012). Ubiquitin-like proteins. *Annual review of biochemistry*, *81*, 323–357. https://doi.org/10.1146/annurev-biochem-093010-153308

45. van Gent, M., Braem, S. G., de Jong, A., Delagic, N., Peeters, J. G., Boer, I. G., Moynagh, P. N., Kremmer, E., Wiertz, E. J., Ovaa, H., Griffin, B. D., & Ressing, M. E.

(2014). Epstein-Barr virus large tegument protein BPLF1 contributes to innate immune evasion through interference with toll-like receptor signaling. *PLoS pathogens*, *10*(2), e1003960. https://doi.org/10.1371/journal.ppat.1003960

46. Walczak, C. P., Leto, D. E., Zhang, L., Riepe, C., Muller, R. Y., DaRosa, P. A., Ingolia, N. T., Elias, J. E., & Kopito, R. R. (2019). Ribosomal protein RPL26 is the principal target of UFMylation. *Proceedings of the National Academy of Sciences of the United States of America*, *116*(4), 1299–1308. https://doi.org/10.1073/pnas.1816202116

47. Wang, Z., Gong, Y., Peng, B., Shi, R., Fan, D., Zhao, H., Zhu, M., Zhang, H., Lou, Z., Zhou, J., Zhu, W. G., Cong, Y. S., & Xu, X. (2019). MRE11 UFMylation promotes ATM activation. *Nucleic acids research*, *47*(8), 4124–4135. https://doi.org/10.1093/nar/gkz110

48. Wang, L., Xu, Y., Rogers, H., Saidi, L., Noguchi, C. T., Li, H., Yewdell, J. W., Guydosh, N. R., & Ye, Y. (2020). UFMylation of RPL26 links translocation-associated quality control to endoplasmic reticulum protein homeostasis. *Cell research*, *30*(1), 5–20. https://doi.org/10.1038/s41422-019-0236-6

49. Watanabe, T., Fuse, K., Takano, T., Narita, Y., Goshima, F., Kimura, H., & Murata, T. (2015). Roles of Epstein-Barr virus BGLF3.5 gene and two upstream open reading frames in lytic viral replication in HEK293 cells. *Virology*, *483*, 44–53. https://doi.org/10.1016/j.virol.2015.04.007

50. Whitehurst, C. B., Ning, S., Bentz, G. L., Dufour, F., Gershburg, E., Shackelford, J., Langelier, Y., & Pagano, J. S. (2009). The Epstein-Barr virus (EBV) deubiquitinating enzyme BPLF1 reduces EBV ribonucleotide reductase activity. *Journal of virology*, *83*(9), 4345–4353. https://doi.org/10.1128/JVI.02195-08

51. Whitehurst, C. B., Vaziri, C., Shackelford, J., & Pagano, J. S. (2012). Epstein-Barr virus BPLF1 deubiquitinates PCNA and attenuates polymerase η recruitment to DNA damage sites. *Journal of virology*, *86*(15), 8097–8106. https://doi.org/10.1128/JVI.00588-12

52. Whitehurst, C. B., Li, G., Montgomery, S. A., Montgomery, N. D., Su, L., & Pagano, J. S. (2015). Knockout of Epstein-Barr virus BPLF1 retards B-cell transformation and lymphoma formation in humanized mice. *mBio*, *6*(5), e01574-15. https://doi.org/10.1128/mBio.01574-15

53. Witting, K. F., & Mulder, M. (2021). Highly Specialized Ubiquitin-Like Modifications: Shedding Light into the UFM1 Enigma. *Biomolecules*, *11*(2), 255. https://doi.org/10.3390/biom11020255

54. Wong, Y., Meehan, M. T., Burrows, S. R., Doolan, D. L., & Miles, J. J. (2022). Estimating the global burden of Epstein-Barr virus-related cancers. *Journal of cancer research and clinical oncology*, *148*(1), 31–46. https://doi.org/10.1007/s00432-021-03824-y

55. Wu, J., Lei, G., Mei, M., Tang, Y., & Li, H. (2010). A novel C53/LZAP-interacting protein regulates stability of C53/LZAP and DDRGK domain-containing

Protein 1 (DDRGK1) and modulates NF-kappaB signaling. *The Journal of biological chemistry*, *285*(20), 15126–15136. https://doi.org/10.1074/jbc.M110.110619

56. Wu, C. C., Peterson, A., Zinshteyn, B., Regot, S., & Green, R. (2020). Ribosome Collisions Trigger General Stress Responses to Regulate Cell Fate. *Cell*, 182(2), 404–416.e14. https://doi.org/10.1016/j.cell.2020.06.006

57. Ylä-Anttila, P., Gupta, S., & Masucci, M. G. (2021). The Epstein-Barr virus deubiquitinase BPLF1 targets SQSTM1/p62 to inhibit selective autophagy. *Autophagy*, *17*(11), 3461–3474. https://doi.org/10.1080/15548627.2021.1874660

58. Yoo, H. M., Kang, S. H., Kim, J. Y., Lee, J. E., Seong, M. W., Lee, S. W., Ka, S. H., Sou, Y. S., Komatsu, M., Tanaka, K., Lee, S. T., Noh, D. Y., Baek, S. H., Jeon, Y. J., & Chung, C. H. (2014). Modification of ASC1 by UFM1 is crucial for ERα transactivation and breast cancer development. *Molecular cell*, *56*(2), 261–274. https://doi.org/10.1016/j.molcel.2014.08.007

59. Zhang, Y., Zhang, M., Wu, J., Lei, G., & Li, H. (2012). Transcriptional regulation of the Ufm1 conjugation system in response to disturbance of the endoplasmic reticulum homeostasis and inhibition of vesicle trafficking. *PloS one*, 7(11), e48587. https://doi.org/10.1371/journal.pone.0048587

60. Zhang, M., Zhu, X., Zhang, Y., Cai, Y., Chen, J., Sivaprakasam, S., Gurav, A., Pi, W., Makala, L., Wu, J., Pace, B., Tuan-Lo, D., Ganapathy, V., Singh, N., & Li, H. (2015). RCAD/Ufl1, a Ufm1 E3 ligase, is essential for hematopoietic stem cell function and murine hematopoiesis. *Cell death and differentiation*, *22*(12), 1922–1934. https://doi.org/10.1038/cdd.2015.51

61. Zhu, H., Bhatt, B., Sivaprakasam, S., Cai, Y., Liu, S., Kodeboyina, S. K., Patel, N., Savage, N. M., Sharma, A., Kaufman, R. J., Li, H., & Singh, N. (2019). Ufbp1 promotes plasma cell development and ER expansion by modulating distinct branches of UPR. *Nature communications*, *10*(1), 1084. https://doi.org/10.1038/s41467-019-08908-5